

July 11

b

A STUDY OF THE EFFECT OF MICA CONTENT
ON THE SECONDARY COMPRESSION OF RESIDUAL SOIL

A THESIS

Presented to

The Faculty of the Graduate Division

by

David Edgar Pauls

In Partial Fulfillment

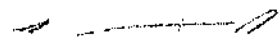
of the Requirements for the Degree


Master of Science in Civil Engineering

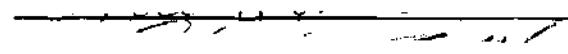
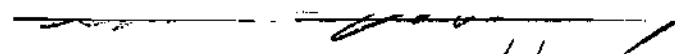
Georgia Institute of Technology

June, 1966

A STUDY OF THE EFFECT OF MICA CONTENT
ON THE SECONDARY COMPRESSION OF RESIDUAL SOIL

Approved: 


Chairman



Date approved by Chairman: 6/2/60

ACKNOWLEDGMENTS

The writer wishes to express his deep gratitude to his thesis advisor, Professor George F. Sowers, and to the members of his reading committee, Dr. N. H. Wade and Dr. C. E. Weaver, for their encouragement and constructive criticisms during this research, and to the National Science Foundation for its financial support during this research and throughout the preceding academic year.

TABLE OF CONTENTS

	Page
ACKNOWLEDGEMENTS	ii
LIST OF TABLES	iv
LIST OF ILLUSTRATIONS	v
SUMMARY	vii
Chapter	
I. INTRODUCTION	1
II. REVIEW OF THE LITERATURE	3
Mica and the Physical Properties of Soil	
Secondary Compression	
X-Ray Diffraction	
III. EQUIPMENT AND PROCEDURE	9
Soil Classification	
Determination of Mica Content	
Determination of Secondary Compression	
IV. SOIL PROPERTIES	15
Source of Samples	
Undisturbed Samples	
Remolded Samples	
V. SUMMARY OF RESULTS	23
VI. DISCUSSION OF RESULTS	28
Determination of Mica Content	
Initial and Primary Compression	
Secondary Compression	
VII. CONCLUSIONS	40
APPENDIX	41
BIBLIOGRAPHY	77

LIST OF TABLES

Table	Page
1. Duration of Loading in Days	14
2. Description and Selected Properties of Undisturbed Samples	16
3. Summary of Test Results	24

LIST OF ILLUSTRATIONS

Figure	Page
1. X-Ray Diffraction Patterns of Sample U4	18
2. X-Ray Diffraction Pattern of Sample U6	19
3. X-Ray Diffraction Pattern of Hornblende Mineral	20
4. Time-Settlement Curve for Sample R7 under 2000 psf.	31
5. Relationship between Mica Content and Compression Index ...	33
6. Relationship between Quartz Content and Compression Index .	34
7. Relationship between Applied Load and Coefficient of Secondary Compression	36
8. X-Ray Diffraction Pattern of Sample U1	42
9. X-Ray Diffraction Pattern of Samples U2 and U3	43
10. Time-Settlement Curves for Sample U1	44
11. Time-Settlement Curves for Sample U2	45
12. Time-Settlement Curves for Sample U3	46
13. Time-Settlement Curves for Sample U4	47
14. Time-Settlement Curves for Sample U5	48
15. Time-Settlement Curves for Sample U6	49
16. Time-Settlement Curves for Sample U7	50
17. Time-Settlement Curves for Sample R1	51
18. Time-Settlement Curves for Sample R2	52
19. Time-Settlement Curves for Sample R3	53
20. Time-Settlement Curves for Sample R4	54
21. Time-Settlement Curves for Sample R5	55
22. Time-Settlement Curves for Sample R6	56

LIST OF ILLUSTRATIONS - Continued

Figure		page
23.	Time-Settlement Curves for Sample R7	57
24.	Time-Settlement Curves for Sample R8	58
25.	Pressure-Settlement Curve for Sample U1	59
26.	Pressure-Settlement Curve for Sample U2	60
27.	Pressure-Settlement Curve for Sample U3	61
28.	Pressure-Settlement Curve for Sample U4	62
29.	Pressure-Settlement Curve for Sample U5	63
30.	Pressure-Settlement Curve for Sample U6	64
31.	Pressure-Settlement Curve for Sample U7	65
32.	Pressure-Settlement Curve for Sample R1	66
33.	Pressure-Settlement Curve for Sample R2	67
34.	Pressure-Settlement Curve for Sample R3	68
35.	Pressure-Settlement Curve for Sample R4	69
36.	Pressure-Settlement Curve for Sample R5	70
37.	Pressure-Settlement Curve for Sample R6	71
38.	Pressure-Settlement Curve for Sample R7	72
39.	Pressure-Settlement Curve for Sample R8	73
40.	Relationship between Mica Content and the Coefficient of Secondary Compression under 1000 psf	74
41.	Relationship between Mica Content and the Coefficient of Secondary Compression under 4000 psf	75
42.	Relationship between Mica Content and the Coefficient of Secondary Compression under 16,000 psf	76

SUMMARY

The effect of mica content on the coefficient of secondary compression of residual micaceous soils in the undisturbed state and in the remolded state was investigated. The undisturbed soils used were saprolites from the Piedmont Province of Georgia, and the remolded soils were saprolites in which the natural mica content was altered by the addition or removal of mica. The soils used were very micaceous silty sands with low plasticity and were classified SM by the Unified soil classification system. The mica content of the undisturbed samples ranged from 8 per cent to 52 per cent, and from 4 per cent to 100 per cent for the remolded samples.

The experimental work consisted of long term consolidation tests and the determination of the mica content, which was done by a combination of magnetic separation, microscopic examination, and x-ray diffraction techniques.

Although the stated purpose of this investigation was to study secondary compression, any division of primary consolidation and secondary compression must be to some extent empirical, and some consideration was given to the effect of the mica content on the primary consolidation characteristics of the soils tested. It was observed that the e -log p curves of the undisturbed samples are curved and approach a straight line under high pressures, and that for a particular source soil the compression index increases with increasing mica content, but that a well defined relationship was not obtained for a group of different soils.

For the remolded soils tested, the coefficient of secondary compression was not significantly affected by the mica content of the soil and for a particular source soil was approximately constant over a wide range of applied pressure.

There was limited evidence that for undisturbed soils the coefficient of secondary compression reaches a maximum which is approximately the same as that obtained with the soil remolded.

A constant value of the coefficient of secondary compression was approached in the undisturbed samples under the same range of loading which produced a straight e -log p curve.

CHAPTER I

INTRODUCTION

Previous work at the Soil Mechanics Laboratory of the Georgia Institute of Technology (1, 2)* indicated that the secondary compression which occurs in residual soils of the Piedmont Province of the eastern United States might be related to the mica content of the soil, but that further work was required to determine the magnitude and nature of this effect.

The Piedmont Province soils which are generally of engineering interest are termed "saprolites", which are soils weathered in place from the underlying igneous and metamorphic rocks and which are soil in texture but have retained the appearance and structure of the parent rock (3). The general characteristics of this class of soil have been described in some detail by Sowers (2, 3). They are characterized by banding due to segregation of minerals in the parent rock. The most common minerals are quartz, mica, partially weathered feldspar, and kaolinite. Ferromagnesium minerals occur in varying amounts. The mica may be distributed throughout the soil in random orientation or may occur in bands of almost pure mica in which the cleavage planes are oriented parallel to the banding. The structure reflects the interlocking of grains of the parent rock. The quartz and mica minerals are resistant to weathering, while the feldspar minerals weather rather

*Numbers in parentheses refer to items in the Bibliography.

rapidly into the kaolinite family of minerals. This gives a framework structure of quartz and mica which retains some of the original interlocking and bonding, with the remaining volume being occupied by kaolinite and the partially weathered feldspar (3).

Although a great deal of work has been done on consolidation and secondary compression of clay, very little has been done on residual soils. The purpose of this research is to study the effect of mica content on the secondary compression of undisturbed and remolded residual soil.

The study of the effect of mica content in soils is complicated by the absence of a quick and reliable procedure for determining the mica content. In addition to more common methods which have been used previously, the use of X-ray diffraction techniques for the quantitative determination of soil minerals, and mica in particular, is considered.

CHAPTER II

REVIEW OF THE LITERATURE

Mica and the Physical Properties of Soil

The effect of mica content on the physical properties of soils was recognized early by Terzaghi, who gave the most important factors influencing the behavior of sands as "grain size, uniformity, volume of voids, and mica content" (see reference 4). At Terzaghi's suggestion, Gilboy (4) conducted a series of cyclic load tests with lateral confinement on mixtures of uniform quartz and muscovite with the mica content varying from 0 to 100 per cent. He found that: (i) the compressibility increases greatly with increasing mica content; (ii) the uncompressed void ratio increased with an increasing percentage of flat grains; and (iii) the pressure-compression diagram of soil under lateral confinement had "a certain definite character, irrespective of the character of the material."

Drawing on his third conclusion, Gilboy attributed the properties of clays to the presence of flat particles and suggested that perhaps the particle shape was more important than its size. He suggested that soils might be classified on the basis of comparison of their compressibility curves to a standard series of compressibility curves for sand-mica mixtures. It might be noted that his suggestion regarding the unimportance of particle size was not well received (5).

Much later, Terzaghi (6) suggested the use of a grain shape factor, F_s , which he designated as the weight per cent of the flaky particles in the soil.

Tate and Larew (7), in investigating the effect of mica content on the resilient rebound of Piedmont residual soils of Virginia, found (as did Gilboy) that the compression and the rebound increased with increasing mica content. They also observed that the mechanism involved was an elastic bending of the flat mica particles. The compression and rebound also was noted to be related to the structure of the soil.

The effect of mica content on the compressibility of compacted micaceous soils was also investigated by McCarthey and Leonards (8), who worked with remolded natural soil and with artificially reconstituted soils. They noted a marked decrease in density with increasing mica content, and gave an empirical equation relating the compression index to the mica content of the non-plastic micaceous soils used.

The compressibility of undisturbed micaceous saprolites was investigated by Clemence (1), who found an increase in compressibility with increasing mica content and noted that in undisturbed samples factors other than mica content affect the compressibility.

Secondary Compression

The literature concerning the secondary compression of soil is voluminous, and only a brief review will be attempted here. Experimental work on secondary compression has been largely confined to plastic clays, although the phenomenon has been noted for such diverse materials as peat (9), volcanic glass of fine sand size (10), shale (11), muskeg (12), rockfill (13), and pure mica (present investigation).

Soon after publication of Terzaghi's classical theory of hydrodynamic consolidation (14), it became apparent that Terzaghi's theory of consolidation did not adequately account for a time-dependent

compression which continued long after the dissipation of a measurable excess hydrostatic pore pressure. Buisman (9) conducted long term (100-500 days) consolidation tests on peat and clay. He found a "secular" or secondary effect in which the settlement was proportional to the logarithm of time (i.e., a straight-line semilog plot), that the secondary effect increased with increasing temperature, that the principle of superposition appeared valid, and that the slope of the secondary compression line was approximately proportional to the applied load. He defined the slope of the void ratio-logarithm of time curve as α_s (which will be designated α in this thesis). He also reported linear time-settlement relationships on semilog plots for the long-term settlement of a road embankment and a levee.

Gray (15), using Boston blue clay, noted that the difference between Terzaghi's theory and actual test results was due to a "secondary time effect" which appeared to be a function of the type and quantity of organic matter in the soil, modified by other considerations. Gray also noted a pronounced temperature effect.

Housel (16) attributed the observed phenomenon to the plastic flow of a plastic material, or to a shearing displacement, but did not explain how this might occur with lateral confinement.

Taylor (17) considered secondary compression to be due to remolding or structural disturbance. "Two possible explanations of the readjustment process are that it may be largely plastic distortion of grain groups, or that it may be mainly the squeezing of water from between very closely spaced flat colloidal sized particles." Edelman (18) attributed secondary compression to a micro-complex of fine soil in the

voids of the larger grains, with the pore water in this micro-complex having a high density and viscosity so "that this water behaves as a very sticky fluid.... The addition of these microsettlements delivers the secular-settlement of the soil." Croce (10), however, obtained a linear semilogarithmic relationship for a sand size volcanic glass soil in spite of the lack of clay size material.

Terzaghi (19) described secondary compression as being the result of a solid layer of adsorbed water which is disturbed by loading and which gradually approaches equilibrium. He cited the results of tests on clays and also on fine, moist quartz powder.

Terzaghi (20) noted that settlement records showed a variety of secondary time effects, and that while settlement is frequently proportional to the logarithm of time, it may also be directly proportional to time. He attributed the first to "the result of grain adjustment under lateral confinement," and the second to the actual squeezing outward of material in thick strata, and cited a case of lateral movement of several feet of an ore yard wall. Examples of both types of settlement of structures may be found in the literature (9, 21, 22, 23, 24, 25).

Taylor (17) noted early (1942) that consolidation "is not independent of the magnitude of effective loading increment, as the Terzaghi theory indicates. Instead consolidation proceeds more slowly for small increments of load." Newland and Allely (26) noted that the slope of the secondary compression line (α) is independent of the pressure increment ratio*, so that larger load increment ratios gave smaller percentages of settlement due to secondary compression.

*The pressure increment ratio is the added load divided by the preceeding total load.

Lo (27) listed three types of curves which he found to be characteristic of secondary compression, and extended his previous theory (28) to include all shapes of secondary compression curves. Leonards and Girault (29) determined that the shape of a time-settlement curve depends on the load increment ratio used, and that small load increment ratios result in large ratios of secondary to primary consolidation. Wahls' (30) work also shows that the slope of the secondary compression line is independent of the load increment ratio, but that the relative proportions attributed to primary and secondary consolidation is related to the load increment ratio. Madhav and Dridharan (31) presented data to show that α is not constant, but that α divided by the load increment is constant (this was also reported by Buisman (9)). Gray (32) reported that for his work, α reaches a maximum at about the preconsolidation load and remains constant thereafter.

Crawford (33) suggested that primary and secondary consolidation are arbitrary divisions of the same process, and offered as evidence the results of consolidation tests performed with a constant strain rate in which excess pore pressure was negligible throughout, and thus "according to the usual definition, experienced secondary consolidation only." Schmertmann (34) maintains that zero pore pressure is insufficient to define the state of secondary compression, and that a condition of constant effective stress is also implied, which condition is not satisfied in strain controlled tests.

Taylor and Merchant (35) proposed a mathematical solution to the problem of soil consolidation which included the effects of secondary compression and which reduced to the Terzaghi theory in the absence of

measurable secondary compression. Several other methods to allow the determination of the end of primary consolidation and to include the effects of secondary compression have been proposed (30, 36, 37, 38).

X-Ray Diffraction

The utility of X-ray diffraction techniques as a method of quantitative analysis of crystalline material was recognized as early as 1919 (39), but the method did not come into its own until about 1945 (40). Alexander and Klug (41) presented the mathematical basis for quantitative analysis of randomly oriented mineral crystals in 1948. More recent work (42) has shown that the theory may also be used for sedimented (oriented) slides of clay minerals. A method of circumventing the problem of obtaining a "standard" of pure material has been presented, but the requirements of this method are too rigorous for application to samples other than those from a single sedimentary deposit.

That the quantitative analysis of clay minerals is still far from an exact science has been vividly demonstrated by Konta (43). Nine clay mineral laboratories were asked to perform a mineralogical analysis of a uniform clay sample. X-ray diffraction was used by all of the laboratories, and eight other methods were used by one or more of the laboratories. The laboratories reported values from 60 to 98 per cent kaolinite, from 5 to 40 per cent minerals of the illite-mica group, 0 to 5 per cent quartz, and 0 to 10 per cent feldspar.

The qualitative analysis of clay minerals is somewhat more advanced, and the literature is extensive (44, 45, 46).

CHAPTER III

EQUIPMENT AND PROCEDURE

Soil Classification

Classification Systems

The soils tested were classified according to the Unified System (47) and the Bureau of Public Roads System (48). Classification by these systems requires a grain size analysis and the liquid and plastic limits. The soil properties were determined from soil trimmings saved from the preparation of the consolidation specimens.

Grain Size Analysis

A combined grain size analysis was used which followed a standard laboratory procedure (49) with two exceptions. The soil was air dried (rather than oven dried) prior to the separation of fine material for the hydrometer analysis, and the fine material was carefully washed through a U.S. Standard No. 325 sieve (0.044 mm.) prior to the hydrometer analysis. The soil coarser than 0.044 mm. was then oven dried and sieved in the usual manner. The necessity of clean material for the magnetic separation (to be discussed later) made this procedure desirable.

Liquid Limit

The liquid limit was determined in accordance with standard laboratory procedures (50) although the tendency of the soil to slide in the cup rather than flow makes the interpretation of the test doubtful (3).

Plastic Limit

The predominance of sand and silt size grains made a valid plastic limit test impossible, since the soil could not be rolled into a fine thread at any water content. The finest threads obtainable were at water contents in excess of the liquid limit (which would lead to negative values of the plasticity index).

Determination of Mica Content

Background

Previous research (1) had indicated that the development of a standard laboratory procedure to determine the mica content of soils was a definite need in research of this type. Common geologic methods such as thin-section inspection with the petrographic microscope require elaborate sample preparations and specialized training on the part of the investigator, and the results obtained are somewhat subjective. Clemence (1) developed a procedure using a combination of magnetic separation, heavy fluid separation, and examination with a petrographic microscope. While a satisfactory determination of mica content could be made in this manner, the time involved was excessive.

Heavy liquid separation was deemed unsatisfactory for this investigation due to the abundance of ferromagnesium minerals, and the methods selected were magnetic separation, microscopic examination, and X-ray diffraction.

Magnetic Separation

Magnetic separation of minerals is based upon the weak magnetic properties which are exhibited by many minerals (51), including mica. Separation of mica from the soil was complicated in the present study by

the presence of other magnetic minerals which could not be separated from the mica by magnetic methods.

A Carpco M-127 magnetic separator which developed a magnetic intensity of 27,000 gauss was provided by the Minerals Engineering Laboratory of the Georgia Institute of Technology. The sieve fractions from the previously conducted sieve analysis were passed through the magnetic separator a sufficient number of times to separate the magnetic and non-magnetic fractions. A clean separation was obtained rapidly for the material coarser than 0.074 mm. (No. 200 sieve), but the finer material could not be satisfactorily separated. Separation proceeded much more readily if the fines (smaller than 0.044 mm) had been washed out. Most of the soils contained magnetic minerals other than mica, and these required the use of a microscope to determine the amount of mica. All separated fractions were examined under a microscope to determine the completeness of separation. The non-magnetic fraction of all soils was very clean, with a typical composition of 95 to 100 per cent quartz, 0 to 5 per cent feldspar, and 0 to 2 per cent mica. The composition of the magnetic fraction was more varied, with typical values of 10 to 100 per cent mica, 0 to 60 per cent ferromagnesium minerals, and 0 to 20 per cent quartz. (The quartz was generally bonded in some manner to a magnetic particle.)

Microscopic Examination

Following separation into magnetic and non-magnetic components, representative samples of each component were examined under a binocular microscope to determine the degree of separation achieved, and a grain count was made of each mineral present. The weight fraction of mica was

determined from the grain count by considering the relative shape and specific gravity of the constituent minerals.

X-Ray Diffraction

Due to the uncertainty which characterizes the use of x-ray diffraction for quantitative analysis of clay minerals at the present time, it was decided to use the x-ray diffraction patterns which were obtained for qualitative and semiquantitative purposes only.

The oriented slides for use in the diffractometer were prepared by pipetting a small amount of suspended soil from the hydrometer analysis cylinder at selected time intervals, so that the approximate maximum size* and the per cent of the sample represented by the soil on the slide would be known. The slides were air dried with no further treatment.

A Norelco (52) system of x-ray diffraction equipment was used which included an x-ray generator producing $\text{CuK}\alpha$ radiation, a wide range goniometer with a proportional counter used with a pulse height analyser, and an electronic circuit panel. The intensity of diffracted radiation was recorded with a strip chart recorder.

The slides were scanned from two degrees (2θ) to 30 degrees (2θ) at a rate of one degree per minute. They were then treated with ethylene glycol and scanned again to ascertain if montmorillonite was present.

* Actually, since hydrometer analysis of particle size is based on Stokes' Law, which gives the velocity of fall of spherical particles, and since many of the soil particles are relatively flat, the apparent size is the diameter of a spherical particle which would fall at the same velocity as the actual soil particle.

Determination of Secondary Compression

The consolidometers were of the fixed-ring type with a sample diameter of 2.375 inches and a height of 1.0 inch. Vertical deflections were measured with micrometer dial gages which read directly to 0.001 inch and could be estimated to 0.0001 inch. Loading was by direct application of weights to a lever arm loading device.

The undisturbed soil samples were carefully trimmed to obtain a good fit in the consolidation ring. Due to the lack of cohesion and the presence of seams of sand size quartz, it was extremely difficult to trim a sample, and as long as eight hours was required to obtain one satisfactory sample. The samples were trimmed directly into the 2.375 inch diameter rings.

The soil samples were placed in the loading device and a seating load of 100 psf was applied. The load was then increased to 500 psf, after which the undisturbed samples were inundated.

The remolded samples were compressed into the consolidation ring in two layers under a static load of 500 psf. They were placed into the loading devices as described above. The remolded samples were then saturated by introducing water into the lower porous stone before they were inundated and loaded to 500 psf.

For the additional loads a load increment ratio of one was used. The loads were left on the sample for varying lengths of time before the next load increment was applied. The length of loading for each sample and each load increment is given in Table 1. Settlement readings were made at 1/4 minute, 1/2 minute, 1 minute, 2 minutes, 4 minutes, 8 minutes, 15 minutes, 30 minutes, 60 minutes, 2 hours, 4 hours, 8 hours, and once

daily thereafter. At the conclusion of the final load increment the loads were removed. The amount of rebound was not determined.

Table 1. Duration of Loading in Days

Sample Number	Applied Load in PSF					
	1000	2000	4000	8000	16,000	32,000
U1	-	1	-	3	3	24
U2	1	1	1	22	-	--
U3	1	1	1	22	-	--
U4	1	1	1	57	1	28
U5	1	1	1	19	-	--
U6	1	1	1	56	1	28
U7	1	1	1	19	-	--
R1	1	8	1	14	1	28
R2	1	8	1	14	1	28
R3	1	8	1	14	1	28
R4	1	8	1	14	1	28
R5	1	8	1	14	1	28
R6	1	8	1	14	1	28
R7	1	8	1	14	1	28
R8	1	8	1	14	1	28

CHAPTER IV

SOIL PROPERTIES

Source of Samples

The soils used in this investigation were saprolites from the Piedmont Province of Georgia. Seven undisturbed samples were tested, and eight remolded samples were prepared and tested. Undisturbed samples U1, U2 and U3 were taken by thin-wall samplers from construction sites in the Atlanta area and were supplied by Law Engineering Testing Company. Sample U1 was taken from a depth of seven feet, and samples U2 and U3 were from the same thin-wall sampler and were taken from a depth of 10 feet. Sample U4 was taken as a shallow sample from a borrow pit in the Atlanta area. The depth below the original ground surface was estimated to be eight feet. Samples U5, U6 and U7 were taken with five inch diameter Shelby tubes from a dam site near West Point, Georgia, and were provided by the Army Corps of Engineers. Samples U5, U6 and U7 were taken from the same borehole at depths of 26, 28 and 30 feet respectively. Traces of the original rock structure were apparent in all of the samples.

Undisturbed Samples

A description of the undisturbed samples, the principal minerals, the mica content, and the classification are given in Table 2. The mineralogy of samples U4 and U6 was considered in more detail than the other samples, as they were used in the preparation of the remolded samples. (Sample U6 may be considered as representative of samples U5

Table 2. Description and Selected Properties of Undisturbed Samples

Sample Number	Description	Principal Minerals	Mica Content	Classification	
				BPR	Unified
U1	Red silty sand highly weathered from schist	Quartz Kaolinite Muscovite	12%	A-5	SM
U2, U3	Reddish-yellow silty sand weathered from gniess, with large amount of sand size mica	Mica Quartz	52%	A-2-5	SM
U4	Red clayey sand weathered from mica schist, with seams of almost 100 per cent mica	Quartz Biotite Kaolinite	43%	A-2-4	SM
U5, U6, U7	Yellow and white silty sand weathered from hornblende gniess	Quartz Hornblende Mica	9% 8% 14%	A-5 A-5 A-2-5	SM SM SM

and U7.)

The soil coarser than 0.044 mm. (U.S. Standard No. 325) of sample U4 was a well graded sand which consisted of a clean angular quartz and a clean golden brown mica (biotite or phlogopite). The soil finer than 0.044 mm. was kaolinite, mica, and mixed layer clay minerals, with little or no quartz. The x-ray diffraction pattern for the soil finer than 0.044 mm is shown in Figure 1. For comparison, the pattern for the "pure" mica (ground from a coarser fraction) is also shown. (It should be noted here that the amount of each component in the sample is not directly proportional to its relative peak height, and that kaolinite has much "stronger" peaks than mica.) Inspection of Figure 1 shows that even the "pure" mica contains some partially weathered kaolinite. The soil sample had a much higher kaolinite content, and also a higher percentage of mixed layer clay minerals.

The mineralogy of sample U6 was more complex. The coarse fraction (larger than 0.044 mm) contained quartz, mica and a hornblende mineral, with some partially weathered feldspar binding the above minerals into small aggregates which would not break apart with gentle rubbing, which is probably due to some remaining bonding of minerals in the parent rock. The hornblende was slightly magnetic, and could not be separated magnetically from the mica. The fine fraction consisted of mica and kaolinite with a trace of quartz. The x-ray diffraction pattern for the finer material is shown in Figure 2. A powder mount x-ray diffraction pattern of the hornblende mineral is shown in Figure 3. The mineral could not be completely separated from the quartz and the quartz diffraction pattern is superimposed, making a precise determination of the mineral difficult.

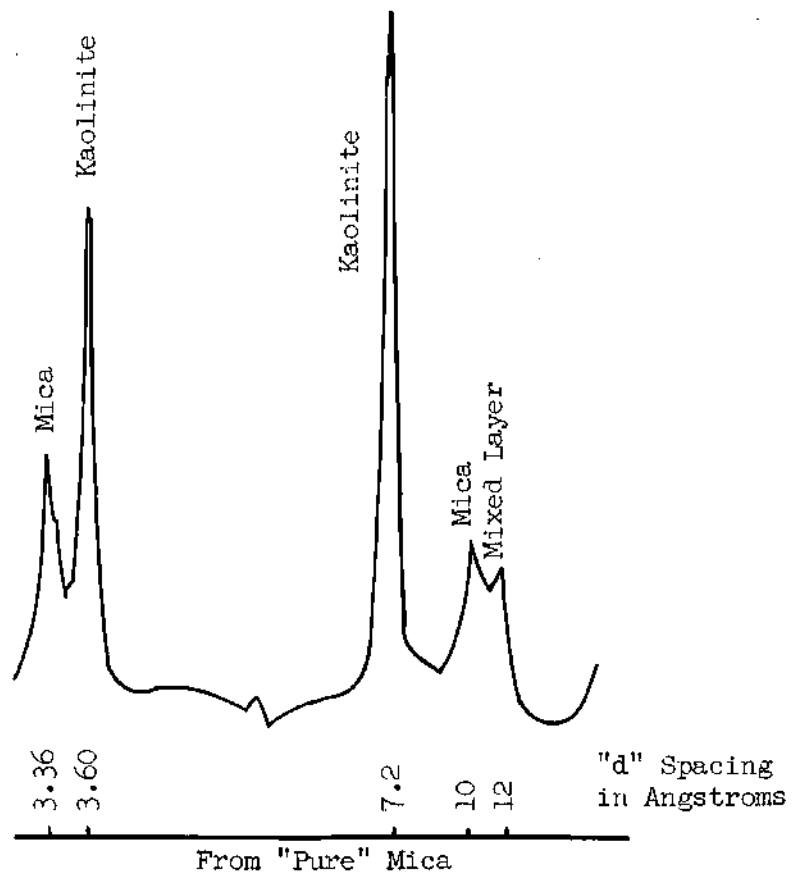
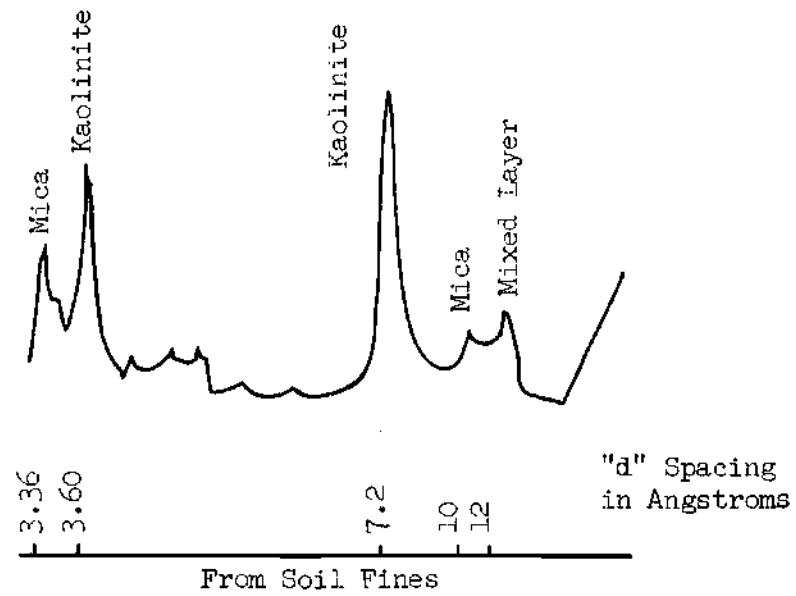


Figure 1. X-ray Diffraction Patterns of Sample U4

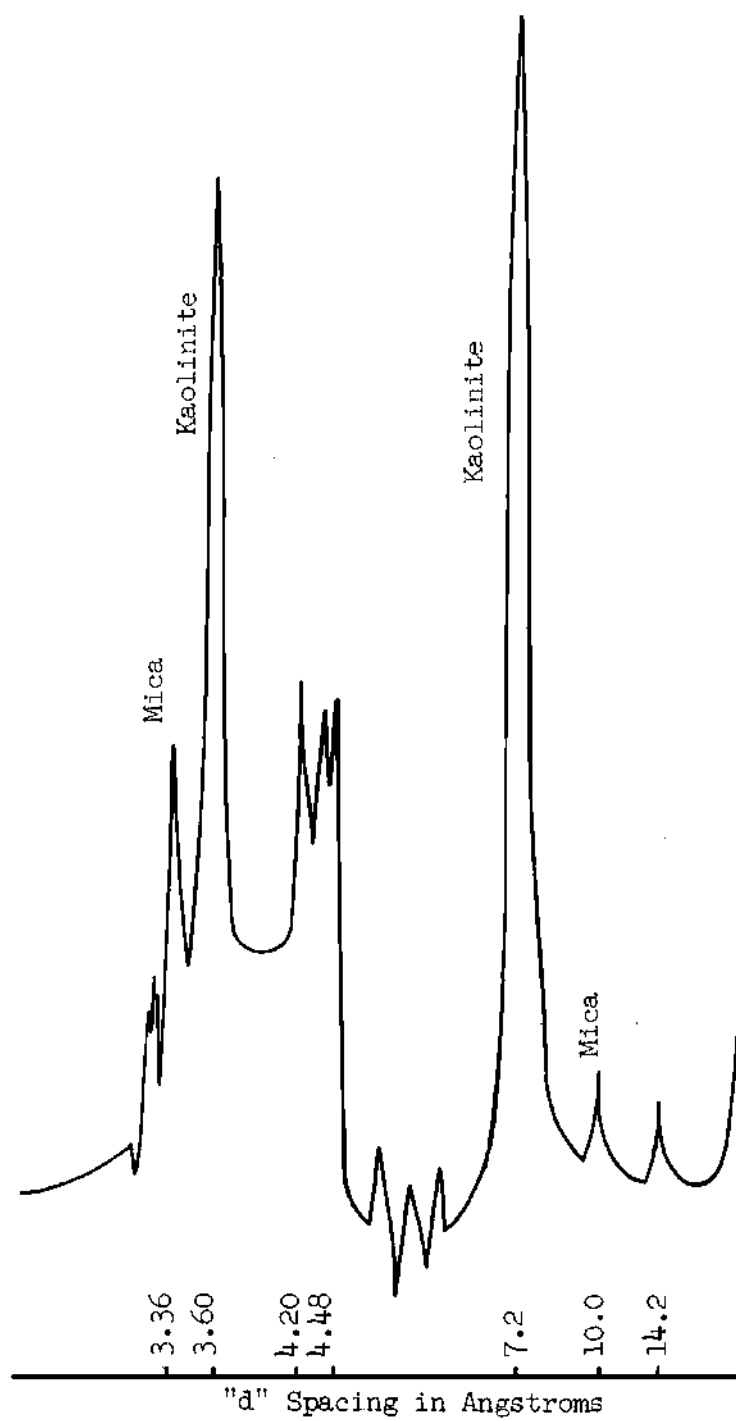


Figure 2. X-ray Diffraction Pattern of Sample U6

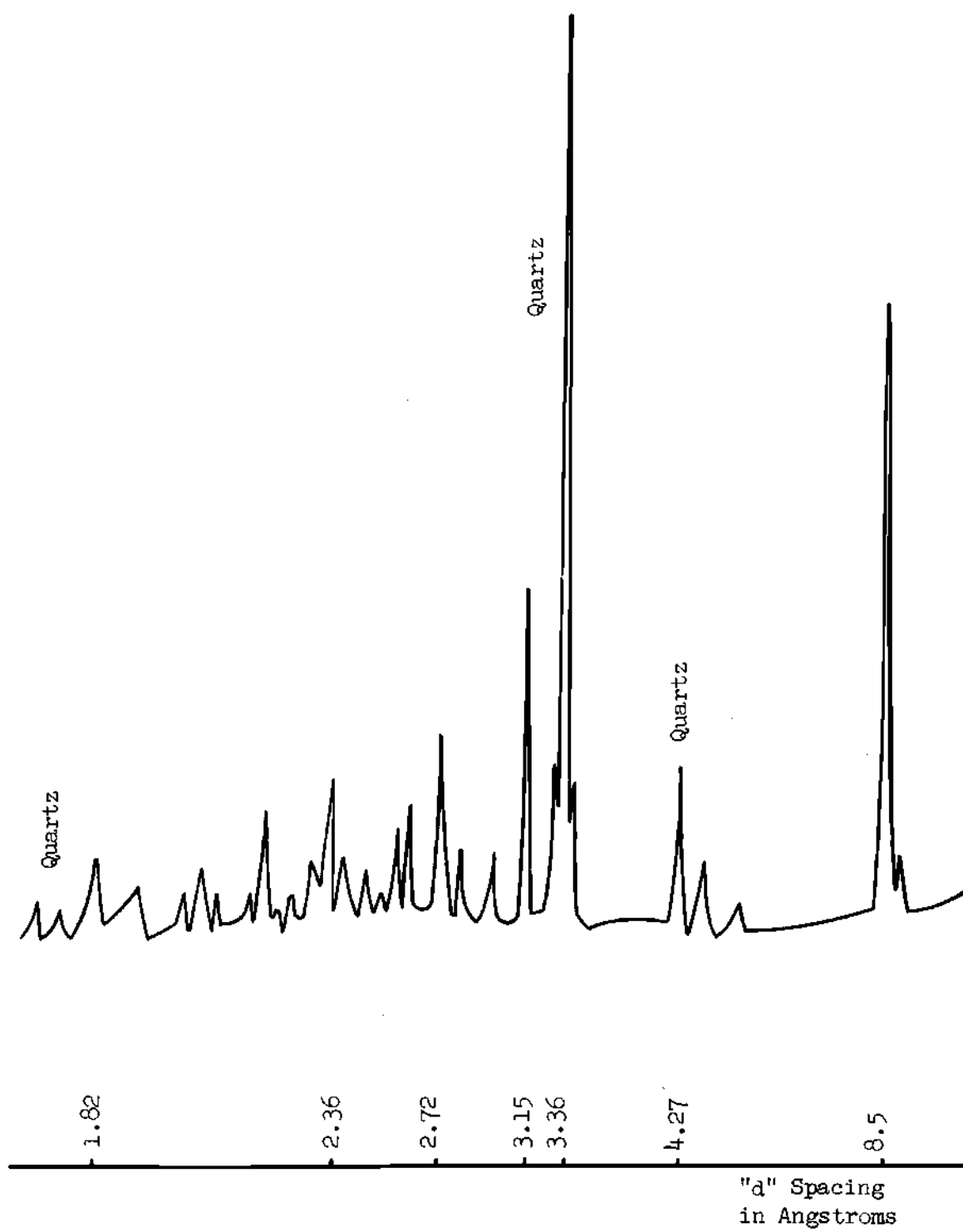


Figure 3. X-ray Diffraction Pattern of Hornblende Mineral

Sample U1 was a highly weathered red silty sand with the coarse fraction containing quartz and mica, and with the fine fraction well weathered into kaolinite with only traces of muscovite and quartz. The x-ray diffraction pattern for the fine fraction is Figure 8 in the Appendix.

Samples U2 and U3 were a highly micaceous silty sand, with the non-mica portion consisting of approximately equal portions of quartz and hornblende in the coarse sand sizes, with the hornblende diminishing and the quartz increasing as the grain size decreased. The silt and clay size material consisted of quartz and a poorly ordered kaolinite. The x-ray diffraction pattern for the fine material in these samples is Figure 9 in the Appendix.

Remolded Samples

The remolded samples were prepared by separating and recombining the minerals of samples U4 and U6. Approximately 1500 grams of soil from the bulk sample of U4 was separated into the fractions coarser and finer than 0.044 mm. by repeated washings through a U.S. Standard No. 325 sieve. The soil coarser than 0.59 mm. (U.S. Standard No. 30 sieve) was discarded. The coarse fraction was a clean mixture of quartz and mica which could be separated very cleanly with the magnetic separator. No dispersant was used in the washing, and the material passing the No. 325 sieve flocculated naturally. This wash water was saved and decanted until a slurry of approximately 0.1 grams of solids per milliliter was obtained.

Samples R1 through R4 were prepared by mixing the quartz and mica in the desired amounts, and adding the proper amount of slurry to give the

same percentage of fines as was present in the undisturbed state. The grading of the quartz was different from that of the mica, and each mineral was added in its original gradation. No mica was added to sample R1, and 10, 20, and 30 per cent mica was added to samples R2, R3, and R4 respectively. The addition of the slurry gave a very wet mixture which was thoroughly mixed and then allowed to air dry to a moisture content of 15 per cent before compacting into the consolidation ring. Sample R5 was pure mica in its original gradation from 0.59 mm. to 0.044 mm., with no fine material added.

Samples R6, R7, and R8 were prepared by a different procedure using soil from the bulk sample of U6 and additional mica from sample U4. The magnetic fraction of sample U6 contained both mica and hornblende which could not be readily separated, and the fine material would not flocculate naturally so a different procedure was desirable. Since the sample contained a relatively small amount of mica, additional mica from sample U4 was added to a homogeneous mixture prepared from the bulk sample of U6. The soil coarser than the No. 30 sieve was discarded, and the additional mica had the same gradation as the mica in sample U6. The final mica content of samples R6, R7, and R8 was 20, 30, and 40 per cent respectively.

CHAPTER V

SUMMARY OF RESULTS

A tabular summary of the results of this investigation is given in Table 3. For each sample under each load increment the following is given: (i) the total load; (ii) the initial void ratio (e_0); (iii) the "corrected one minute void ratio" (e_1), which will be explained in Chapter VI; (iv) the change in void ratio for the first minute ($\Delta e = e_0 - e_1$); (v) the slope of the void ratio versus logarithm of time curve (α); and (vi) the dimensionless ratio $\Delta e/\alpha$. The compression index (C_c) is also given for the samples which were loaded heavily to give a well defined compression index.

Table 3. Summary of Test Results

Sample Number	Load in PSF	Initial Void Ratio (e_0)	Corrected One Minute Void Ratio (e_1)	Initial Void Ratio Change ($\Delta e = e_0 - e_1$)	Coefficient of Secondary Compression (α)	$\Delta e / \alpha$	Compression Index (C_c)
U1	2000	0.700	0.691	0.009	-0.0004	25	0.274
	8000	0.690	0.654	0.036	-0.0017	21	
	16000	0.648	0.622	0.026	-0.0018	14	
	32000	0.615	0.580	0.035	-0.0026	13	
U2	1000	1.417	1.392	0.025	-0.0020	12	
	2000	1.385	1.347	0.038	-0.0025	15	
	4000	1.339	1.289	0.050	-0.0036	16	
	8000	1.278	1.207	0.071	-0.0077	9	
U3	1000	1.618	1.597	0.021	-0.0023	9	
	2000	1.589	1.552	0.037	-0.0021	18	
	4000	1.546	1.500	0.045	-0.0031	14	
	8000	1.491	1.411	0.081	-0.0113	7	
U4	1000	0.836	0.829	0.007	-0.0007	10	
	2000	0.827	0.816	0.011	-0.0006	18	
	4000	0.814	0.794	0.019	-0.0009	21	
	8000	0.791	0.751	0.040	-0.0017	24	
	16000	0.743	0.673	0.069	-0.0026	26	
	32000	0.665	0.586	0.079	-0.0032	24	
U5	1000	1.235	1.226	0.008	-0.0013	6	
	2000	1.222	1.198	0.024	-0.0026	9	
	4000	1.189	1.146	0.043	-0.0064	7	
	8000	1.126	0.975	0.151	-0.0109	14	

Table 3. Summary of Test Results (Continued)

Sample Number	Load in PSF	e_o	e_1	Δe	α	$\Delta e/\alpha$	C_c
U6	1000	1.335	1.308	0.026	-0.0034	7	0.516
	2000	1.297	1.256	0.041	-0.0059	7	
	4000	1.237	1.167	0.070	-0.0102	7	
	8000	1.135	1.031	0.104	-0.0125	8	
	16000	0.918	0.871	0.047	-0.0121	-	
	32000	0.832	0.716	0.117	-0.0114	10	
U7	1000	1.267	1.247	0.020	-0.0021	10	
	2000	1.236	1.209	0.027	-0.0045	6	
	4000	1.194	1.135	0.059	-0.0095	6	
	8000	1.105	1.011	0.094	-0.0132	7	
R1	1000	1.109	1.023	0.087	-0.0016	54	0.25
	2000	1.018	0.942	0.076	-0.0015	51	
	4000	0.936	0.872	0.063	-0.0031	20	
	8000	0.864	0.804	0.060	-0.0041	15	
	16000	0.779	0.730	0.050	-0.0045	11	
	32000	0.716	0.650	0.066	-0.0048	14	
R2	1000	1.198	1.097	0.101	-0.0023	43	0.29
	2000	1.090	0.999	0.091	-0.0018	50	
	4000	0.895	0.886	0.009	-0.0013	-	
	8000	0.882	0.822	0.060	-0.0030	20	
	16000	0.809	0.739	0.070	-0.0039	18	
	32000	0.728	0.651	0.077	-0.0039	20	

Table 3. Summary of Test Results (Continued)

Sample Number	Load in PSF	e_o	e_1	Δe	α	$\Delta e/\alpha$	C_c
R3	1000	1.364	1.253	0.111	-0.0014	80	0.33
	2000	1.249	1.150	0.100	-0.0020	50	
	4000	1.142	1.050	0.092	-0.0021	44	
	8000	1.044	0.951	0.093	-0.0024	39	
	16000	0.940	0.854	0.086	-0.0040	21	
	32000	0.843	0.750	0.093	-0.0038	24	
R4	1000	1.374	1.261	0.113	-0.0015	75	0.38
	2000	1.256	1.138	0.118	-0.0019	62	
	4000	1.131	1.025	0.105	-0.0023	46	
	8000	1.019	0.911	0.108	-0.0025	43	
	16000	0.900	0.803	0.097	-0.0036	27	
	32000	0.793	0.690	0.103	-0.0032	31	
R5	1000	2.470	2.336	0.133	-0.0060	22	0.81
	2000	2.317	2.177	0.140	-0.0088	16	
	4000	2.098	1.972	0.126	-0.0092	14	
	8000	1.943	1.747	0.196	-0.0105	18	
	16000	1.700	1.505	0.195	-0.0096	21	
	32000	1.475	1.254	0.221	-0.0089	25	
R6	1000	1.917	1.778	0.139	-0.0120	11	0.66
	2000	1.742	1.590	0.152	-0.0122	12	
	4000	1.542	1.392	0.149	-0.0134	11	
	8000	1.353	1.188	0.165	-0.0128	13	
	16000	1.133	0.976	0.157	-0.0114	14	
	32000	0.941	0.802	0.139	-0.0107	13	

Table 3. Summary of Test Results (Continued)

Sample Number	Load in PSF	e_o	e_1	Δe	α	$\Delta e/\alpha$	C_c
R7	1000	2.190	2.102	0.088	-0.0109	8	0.69
	2000	2.069	1.917	0.152	-0.0119	13	
	4000	1.869	1.715	0.153	-0.0133	12	
	8000	1.676	1.505	0.171	-0.0132	13	
	16000	1.444	1.294	0.151	-0.0126	12	
	32000	1.255	1.098	0.157	-0.0114	14	
R8	1000	2.029	1.888	0.141	-0.0102	14	0.69
	2000	1.856	1.693	0.162	-0.0128	13	
	4000	1.641	1.487	0.155	-0.0130	12	
	8000	1.447	1.270	0.177	-0.0134	13	
	16000	1.211	1.053	0.158	-0.0115	13	
	32000	1.017	0.859	0.158	-0.0109	15	

CHAPTER VI

DISCUSSION OF RESULTS

Determination of Mica Content

The determination of the mica content of the soil was one of the major experimental problems of this research. The method used for the coarse fraction is believed to furnish an estimate of the total mica content which is accurate to within 5 per cent. The presence of other slightly magnetic material in the soil made it necessary to resort to a microscopic grain counting procedure which was relatively time consuming but which gives a high degree of accuracy if the samples are representative of the soil mass. If mica is the only magnetic mineral present the amount of mica can be obtained directly from the magnetic separation, with a microscopic examination used only to assure completeness of separation.

The determination of the mica content of soil in the size range of silt and clay is much less precise, but the importance of this is reduced by two factors. One factor is that the soil in this size range is a relatively small portion of the total soil for the sample studied. The other, and more important, factor is that the smaller grain sizes are more susceptible to chemical weathering and the mica in this size range is rapidly weathered into kaolinite. This factor is evident from the x-ray diffraction patterns which all show an abundance of kaolinite and a deficiency of mica in the fine fraction of the samples. This rapid weathering into kaolinite should not be considered as a general phenomenon, however, as other

climatic and topographic conditions may yield entirely different results.

One problem in attempting to relate the mica content of soil to its physical properties is the unknown effect of the presence of bulky stacks of particles of mica which have not weathered or broken into thin sheets. These particles are most common in the size range of medium sand and were not found below the largest silt size. If the effect of mica on the soil's physical properties is attributed to the flaky shape of the particles, the bulky books of mica would not contribute fully to this effect, while on the other hand their elastic properties would certainly be different from those of a grain of quartz or feldspar.

Initial and Primary Compression

Although the intent of this research was to study secondary compression, it is impossible to completely separate the effect of secondary compression from that of primary consolidation. If secondary compression may be defined as a time-dependent compression which occurs under constant effective stress and with zero or negligible (or nonmeasurable) pore pressure, it is necessary to determine the point at which the pore pressure reaches zero, which is the same problem as determining the end of primary consolidation. If secondary compression is taken as that compression which gives a straight line when plotted as settlement versus logarithm of time, the problem is again that of determining the time (and the settlement) which marks the end of primary consolidation and the beginning of secondary compression. In the author's opinion, primary consolidation and secondary compression are two stages of a single compression mechanism, in which the first stage is characterized by a

retarding effect due to the expulsion of pore water, and the second stage is characterized by the absence of hydrodynamic effects.

Since the consolidometers used were not equipped to measure the pore pressure of the soil, the end of the initial and primary consolidation stage and the beginning of secondary compression was determined by an arbitrary procedure. Due to the high permeability of the soil the hydrodynamic or primary consolidation occurred very rapidly, usually in one or two minutes, so that the shape of the void ratio versus logarithm of time curve for primary consolidation could not be accurately determined. This was immediately followed by a linear void ratio versus logarithm of time relationship. The typical shape of the e -log t curves is shown in Figure 4, which is the e -log t curve for sample R7 under a 2000 psf load. It is apparent that the settlements after one minute are very close to a straight line. A least squares fit was applied to the data points, and then each point was checked for fit to the computed line. Points varying more than 0.001 were discarded and a least squares fit applied to the remaining points. This process was repeated until no point varied from the computed line by more than 0.001. The intercept of this line with the one minute abscissa was taken as the end of primary consolidation, and the slope of the line taken as the coefficient of secondary compression, α . The one minute intercept will be termed the "corrected one minute void ratio" (e_1) in this discussion. The above computations were performed by a Burroughs B-5500 digital computer from an ALGOL 60 program written by the author. Usually only the one minute point and occasionally the two minute point would be discarded, with the corrected one minute void ratio varying from the observed one minute point a maximum of 0.005 and an average of

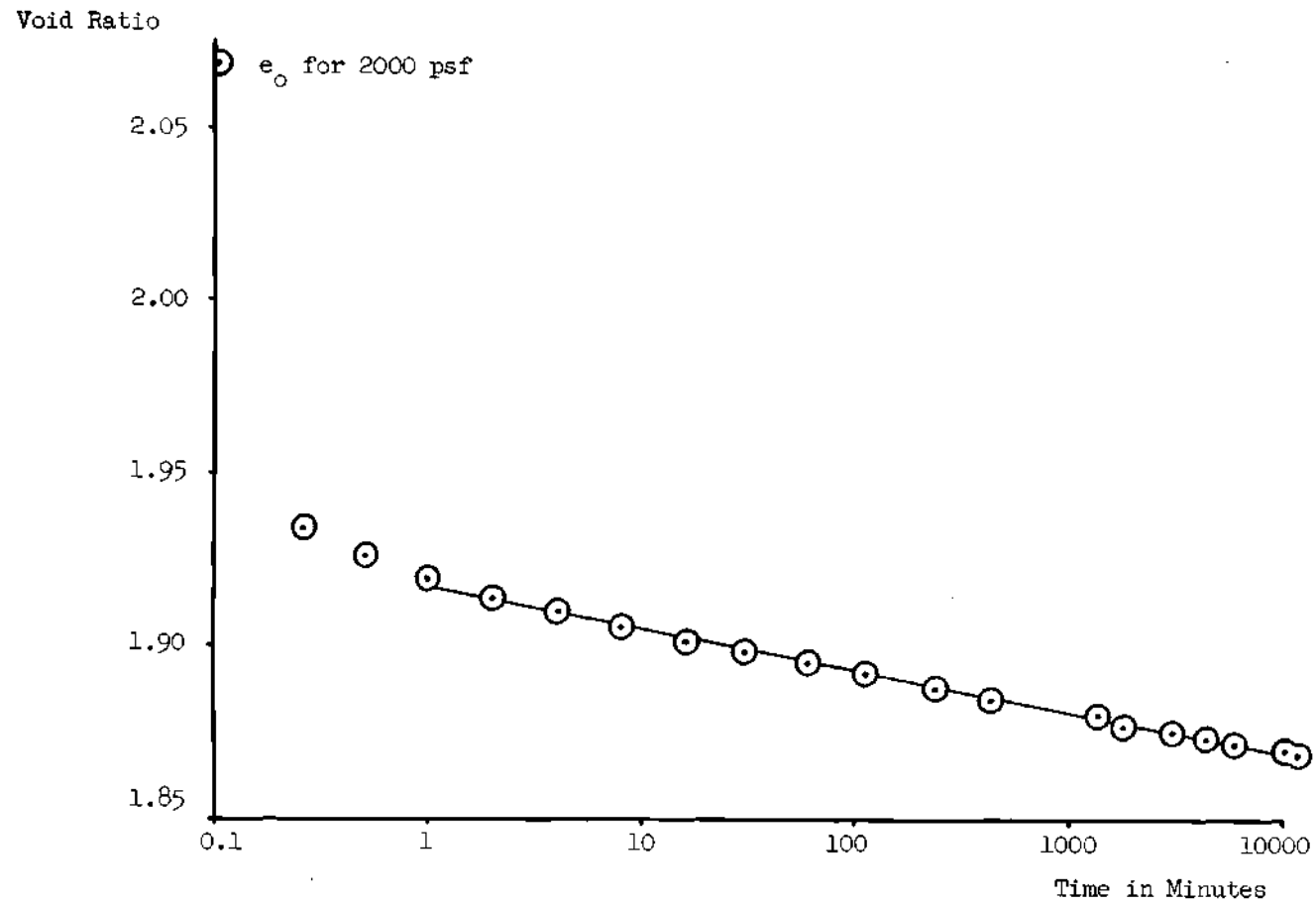


Figure 4. Time Settlement Curve for Sample R7 under 2000 psf

0.0011. Due to the rapid primary consolidation and the close fit of the data points to the computed line in the secondary compression phase, large scale time-settlement curves were not individually plotted. The time-settlement curves for all load increments on each sample were combined to illustrate the relative contribution of initial, primary, and secondary compression to the total soil settlement (Figures 10 to 24 in the Appendix).

The extremely rapid primary consolidation made it impractical to determine the coefficient of consolidation, c_v . Void ratio versus logarithm of pressure curves were obtained using the corrected one minute void ratio (Figures 25 to 39 in the Appendix). The undisturbed samples gave rounded e-log p curves which had some tendency to become straight at higher pressures. Only two undisturbed samples were loaded heavily enough to develop a significant straight line portion of the e-log p curve. All of the undisturbed samples exhibited curves indicating some degree of pre-consolidation. This apparent pre-consolidation is believed to be due to residual stresses from the shearing and cooling of the parent rock, although Vargas (53) found evidence of true pre-consolidation in residual soils from depths greater than 25 feet.

The remolded samples gave straight lines for the virgin compression curve. The relationship between the compression index and mica content is shown on Figure 5. The compression index increases with increasing mica content for a particular source soil, but the correlation between different source soils is not so well defined. It is interesting to note that for the remolded soils tested, a better relationship is obtained between the compression index and the quartz content than is obtained for the mica content, as may be seen by comparison of Figures 5 and 6. This could

Compression
Index

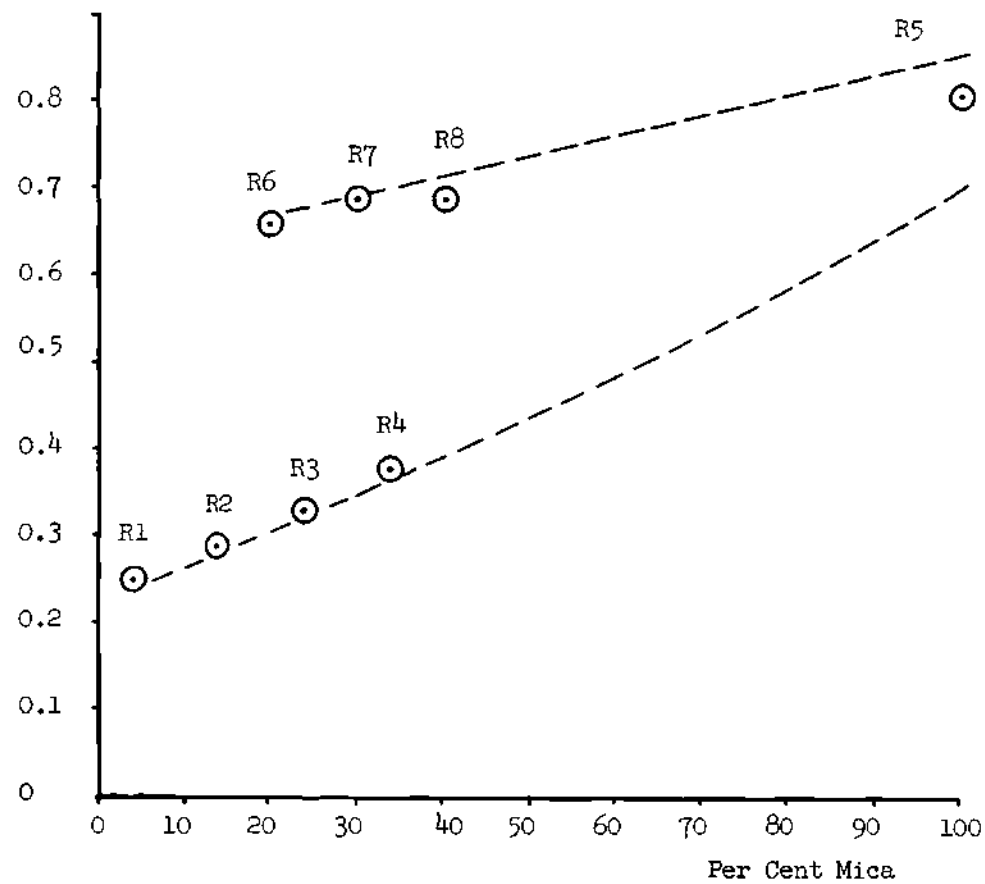


Figure 5. Relationship between Mica Content and Compression Index

Compression
Index

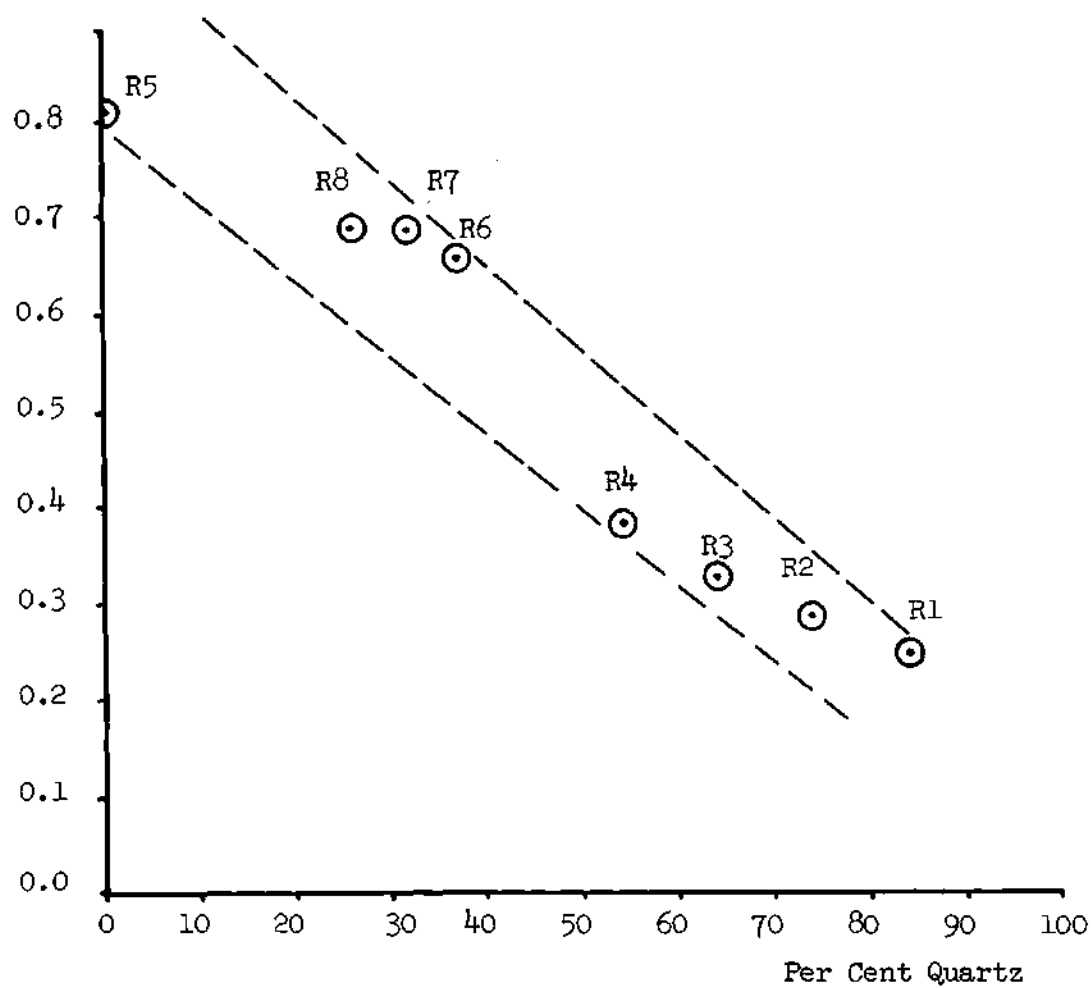


Figure 6. Relationship between Quartz Content and Compression Index

possibly be due to the flaky nature of the major portion of non-quartz minerals, such as kaolinite, which is the third most abundant mineral present in the soil samples. Additional research would be required to determine if this is a significant factor.

Secondary Compression

The coefficient of secondary compression, α , varies over a wide range of values for the undisturbed samples (Table 3 and Figure 7), but generally increases with increasing load. Although α also varies over a wide range of values for the remolded samples, the range of values of α for a particular source soil is relatively narrow for a wide range of mica contents, as may be seen by comparison of the curves (Figure 7) for samples R1, R2, R3, and R4, which have mica contents ranging from 4 to 34 per cent, and the curves for samples R6, R7, and R8, which have mica contents ranging from 20 to 40 per cent. Sample R5, which is the pure mica which was added to the other samples, has an intermediate range of values between the highest and lowest values of α which were obtained. Graphs of α versus mica content for representative loadings are given in the Appendix (Figures 40 to 42). These results indicate that the coefficient of secondary compression for the remolded soils which were tested is not significantly affected by the mica content of the soil.

Several undisturbed soils exhibit a relatively large increase at some particular load increment, which suggests that perhaps much of the original bonding has been destroyed by that particular load increment, and the soil approaches the value of α which it would have in the remolded state. This is supported by the results of the tests on the remolded

Coefficient of
Secondary Compression, α

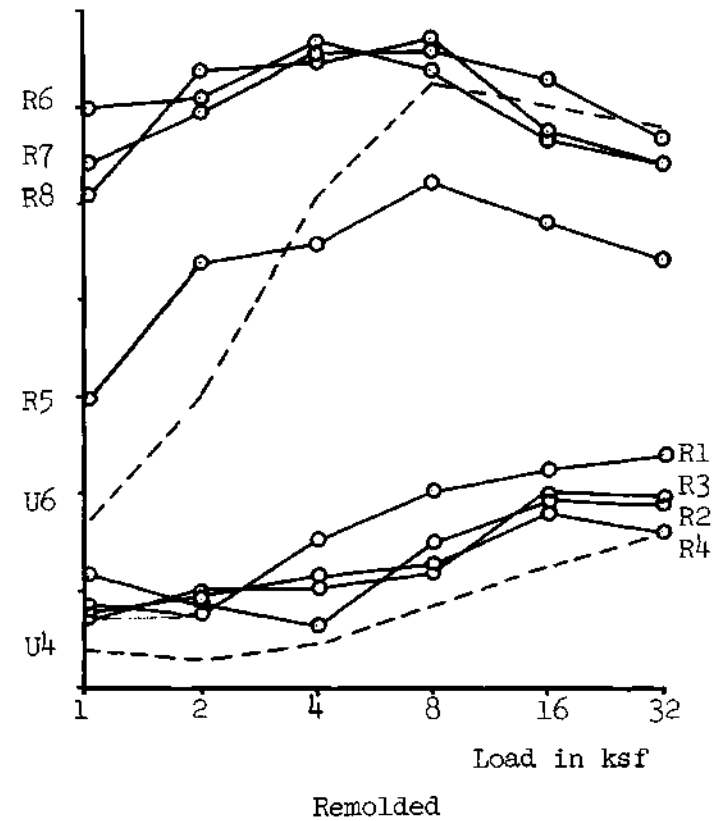
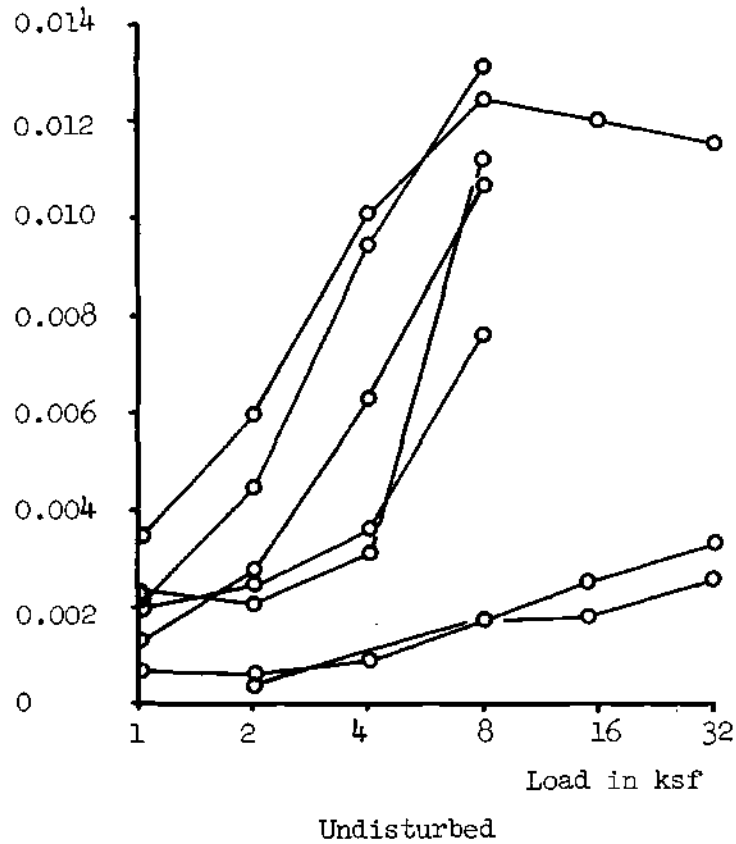


Figure 7. Relationship between Applied Load and Coefficient of Secondary Compression

samples, which give values of α with a much narrower range for a particular sample, and with the value of α reaching a maximum and decreasing slightly at the higher pressures. The maximum values of α for the undisturbed samples approach those obtained for the remolded samples. A comparison between the values of α for the remolded samples and the undisturbed parent material is interesting. The curve on Figure 7 for sample U⁴ lies slightly below those of samples R¹, R², R³, and R⁴ over the entire range of loading, but approaches the maximum value of the remolded samples under the larger load increments. A similar relationship may be noted between undisturbed samples U⁵, U⁶, and U⁷ and remolded samples R⁶, R⁷, and R⁸. The undisturbed samples show increasing values of α with increasing load, and reach a maximum value which is very close to that obtained with the remolded samples.

The wide range of values of α obtained for individual undisturbed samples makes it difficult to relate α to any other soil property, but if one accepts the very limited evidence presented here that α for the undisturbed soils tested reaches a maximum value which is relatively independent of the mica content, and which may be determined from the soil in a disturbed state, it may also be concluded that α of the same source soil in the undisturbed state is not significantly affected by the mica content.

If the maximum value of α is produced by obtaining a complete disruption of the bonding which has remained from the parent rock, one might expect that so important a change would be reflected in other behavior of the soil. The undisturbed soils which exhibit a relatively constant value of α for the last two or three load increments also exhibit a linear e -log p relationship over the same range of applied

pressure, while the remaining soils have a more rounded e -log p curve. The remolded samples exhibited both a straight line e -log p curve and an approximately constant value of α . This indicates to the writer that for the residual soils tested, both the extent of initial plus primary consolidation under applied loads (as reflected in the e -log p curves), and the rate of secondary compression are related to the extent to which the original bonding between the minerals in the parent rock have been broken. A different, but closely related, factor is the extent to which the original minerals have been altered by weathering. Additional research into this mechanism may prove fruitful.

Since an attempt to determine primary and secondary compression will ultimately lead to a predicted settlement of a structure, the effect of both must be considered. To establish a means of comparing the amount of immediate and primary consolidation with the amount which may be attributed to secondary compression, the change in void ratio for the first minute of loading was divided by the coefficient of secondary compression, α . While this dimensionless ratio gives some indication of the relative importance of the two compression phases, it does not give the relative amounts of each, since α is for only one logarithmic time cycle, and the relative importance of each depends on the time involved. The value of this ratio varied from 6 to 26 for the undisturbed samples and from 8 to 80 for the remolded samples. The values for the undisturbed samples give settlements due to secondary compression ranging from about 20 to 50 per cent of the total settlement for the first two years of loading, which is certainly a significant portion of the settlement. Since the initial and primary consolidation occur quite rapidly, it is probable

that the major portion of settlement due to them will occur during construction and that practically all settlement after completion of construction will be due to secondary compression.

CHAPTER VII

CONCLUSIONS

1. The mica content of the soils tested may be determined to within 5 per cent by a combination of magnetic separation, microscopic examination, and x-ray diffraction analysis.
2. The e -log p curves of the undisturbed samples of the residual micaceous silty sands tested are curved and approach a straight line under pressures greater than 4000 to 8000 psf.
3. For a particular soil the compression index increases with increasing mica content, but a well-defined relationship was not obtained for a group of different soils.
4. For remolded soils the coefficient of secondary compression is not significantly affected by the mica content of the soil and is approximately constant over a wide range of applied pressures for a particular soil.
5. There is limited evidence that for undisturbed soils the coefficient of secondary compression reaches a maximum which is approximately the same as that obtained with the same soil remolded.
6. The undisturbed samples approach a constant value of the coefficient of secondary compression under the applied pressures which produce a straight e -log p curve.

APPENDIX

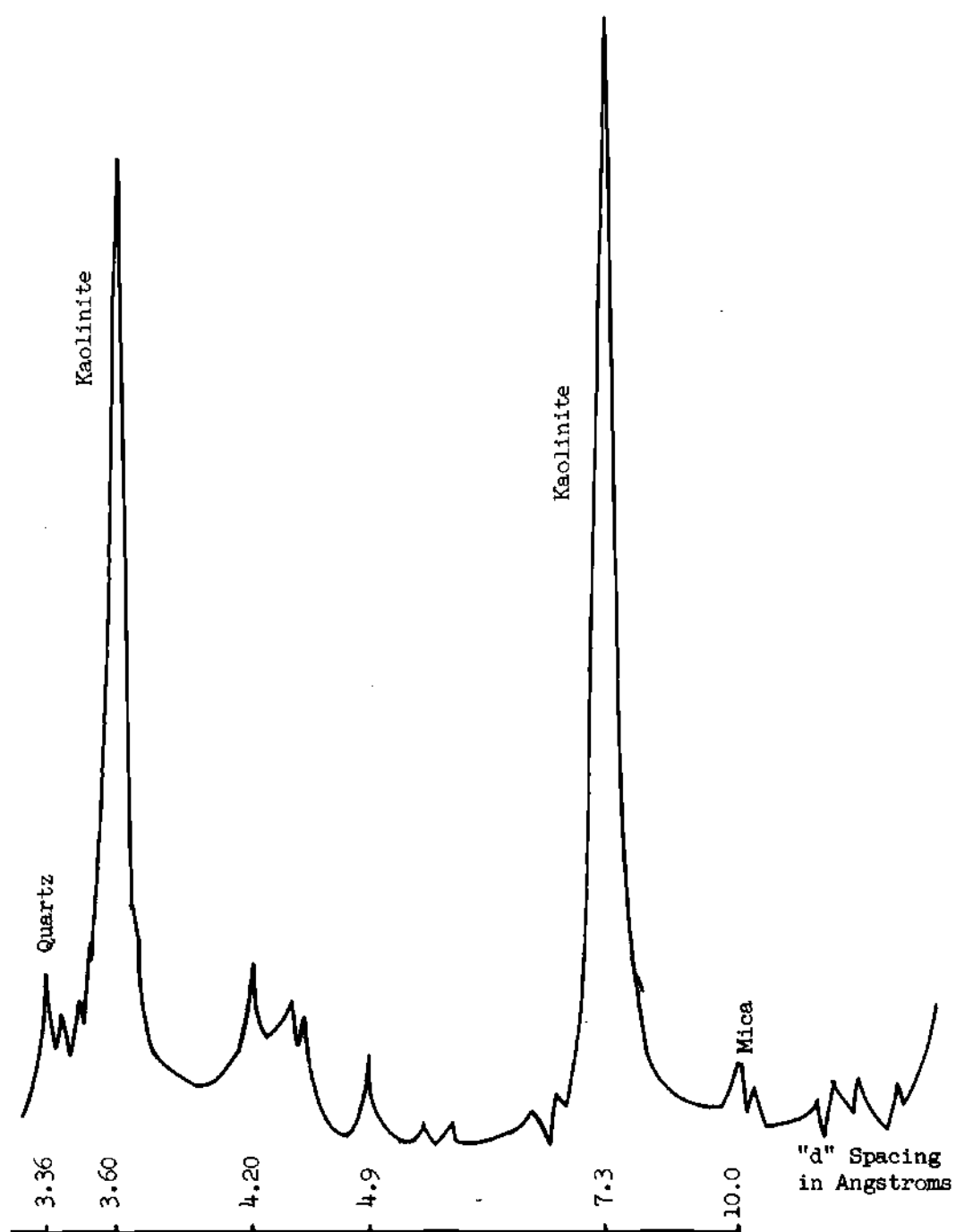


Figure 8. X-ray Diffraction Pattern of Sample U1

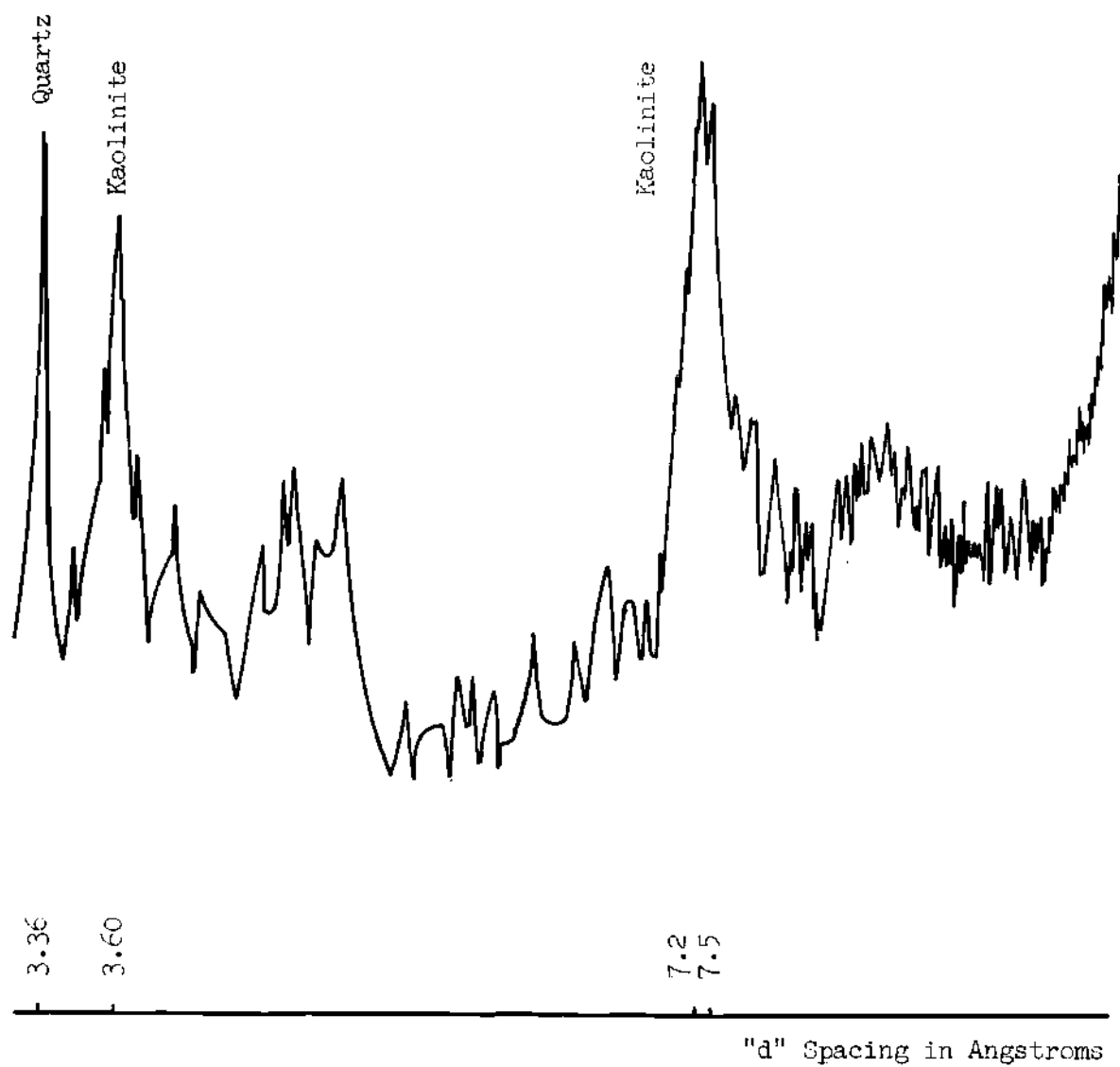


Figure 9. X-ray Diffraction Pattern of Samples U2 and U3

Void
Ratio

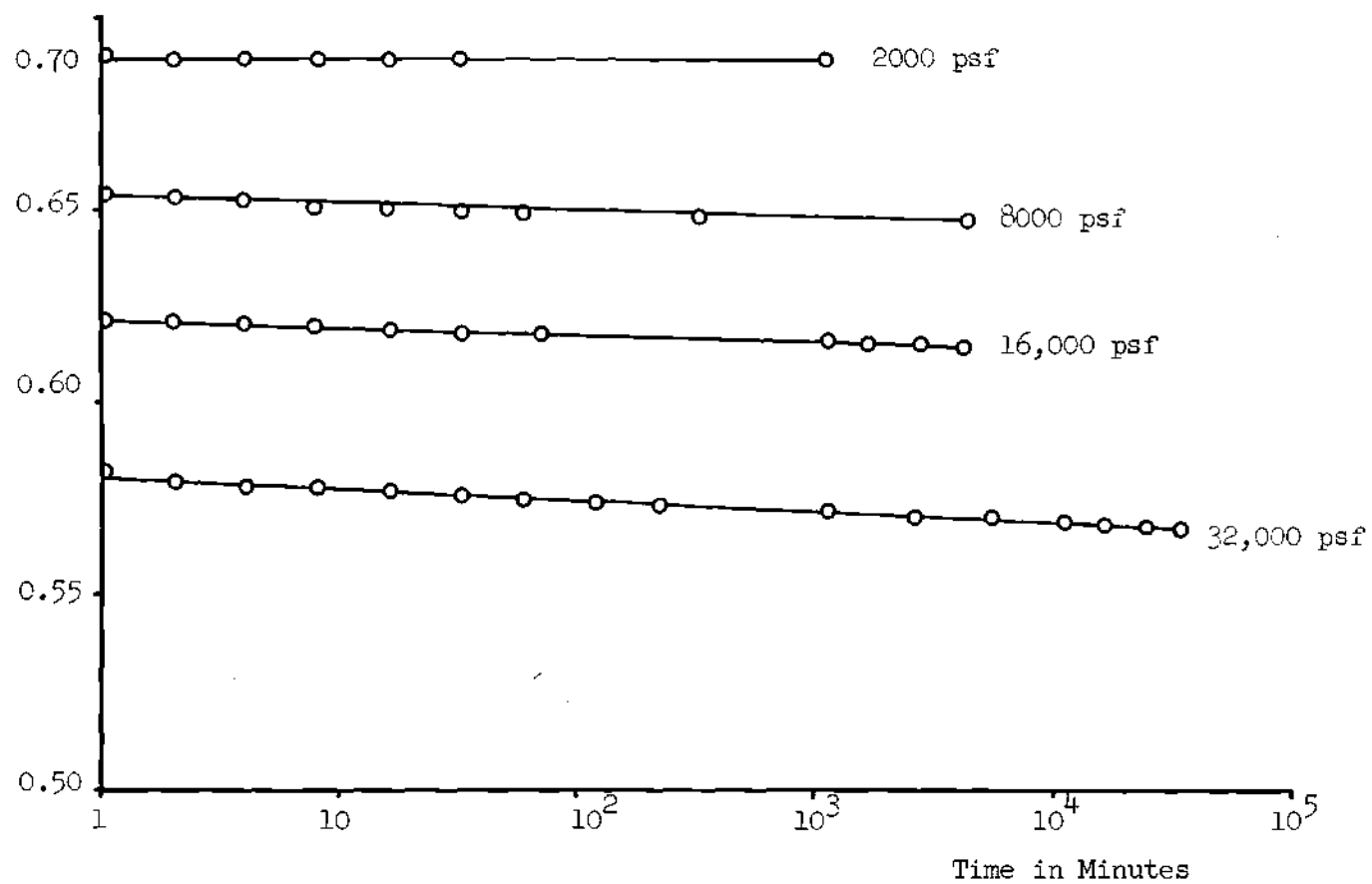


Figure 10. Time-Settlement Curves for Sample U1

Void
Ratio

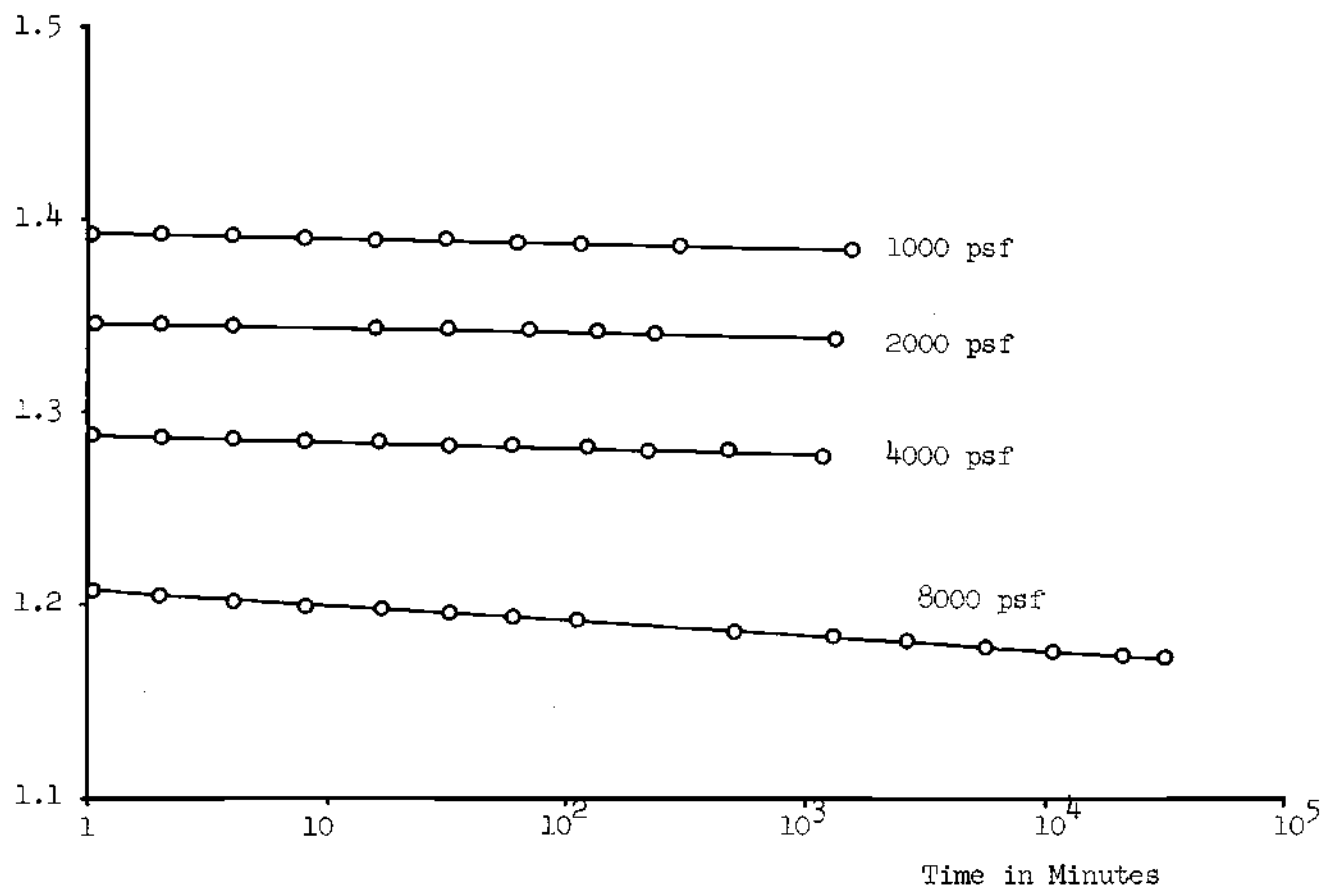


Figure 11. Time-Settlement Curves for Sample U2

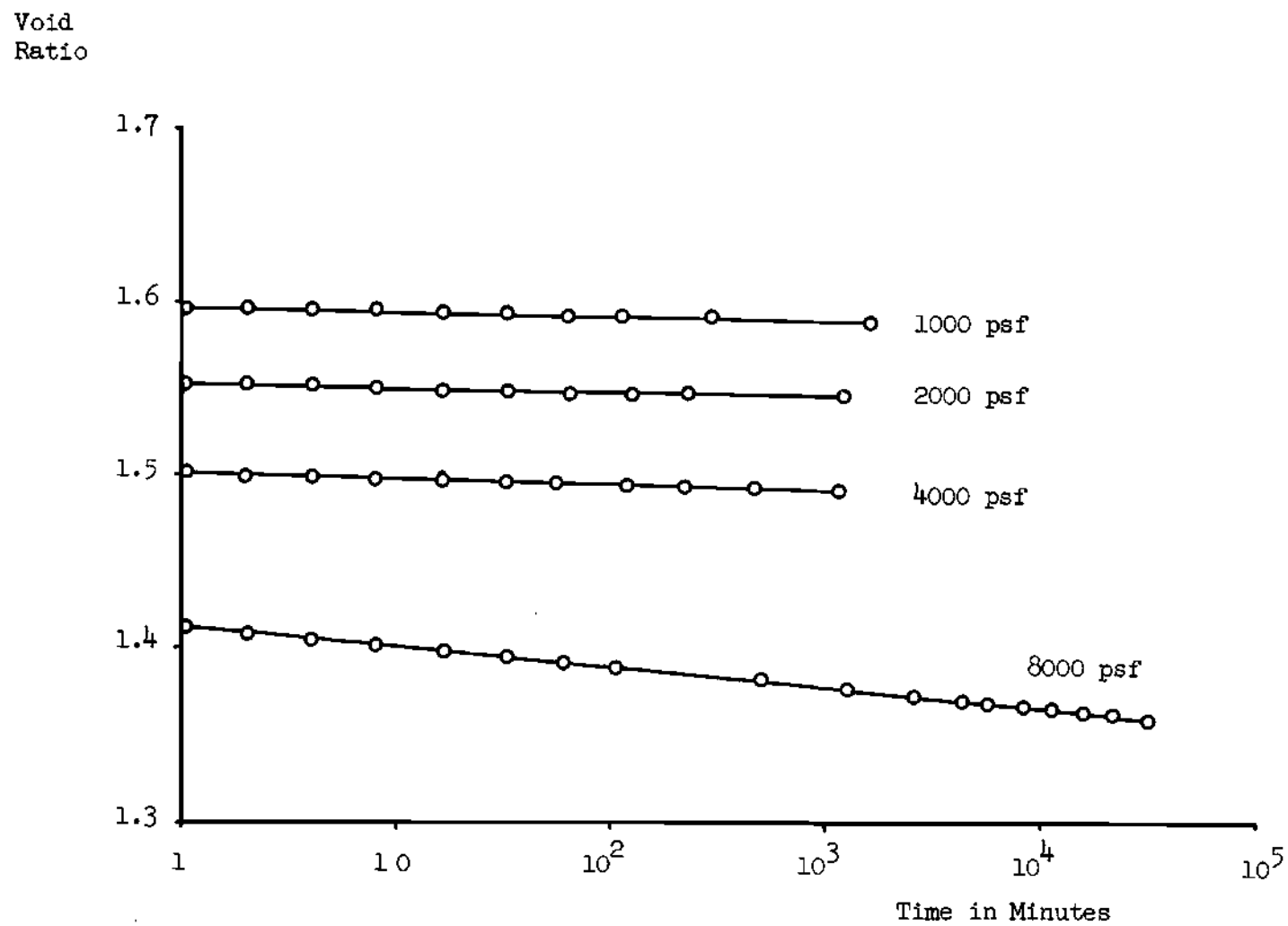


Figure 12. Time-Settlement Curves for Sample U3

Void
Ratio

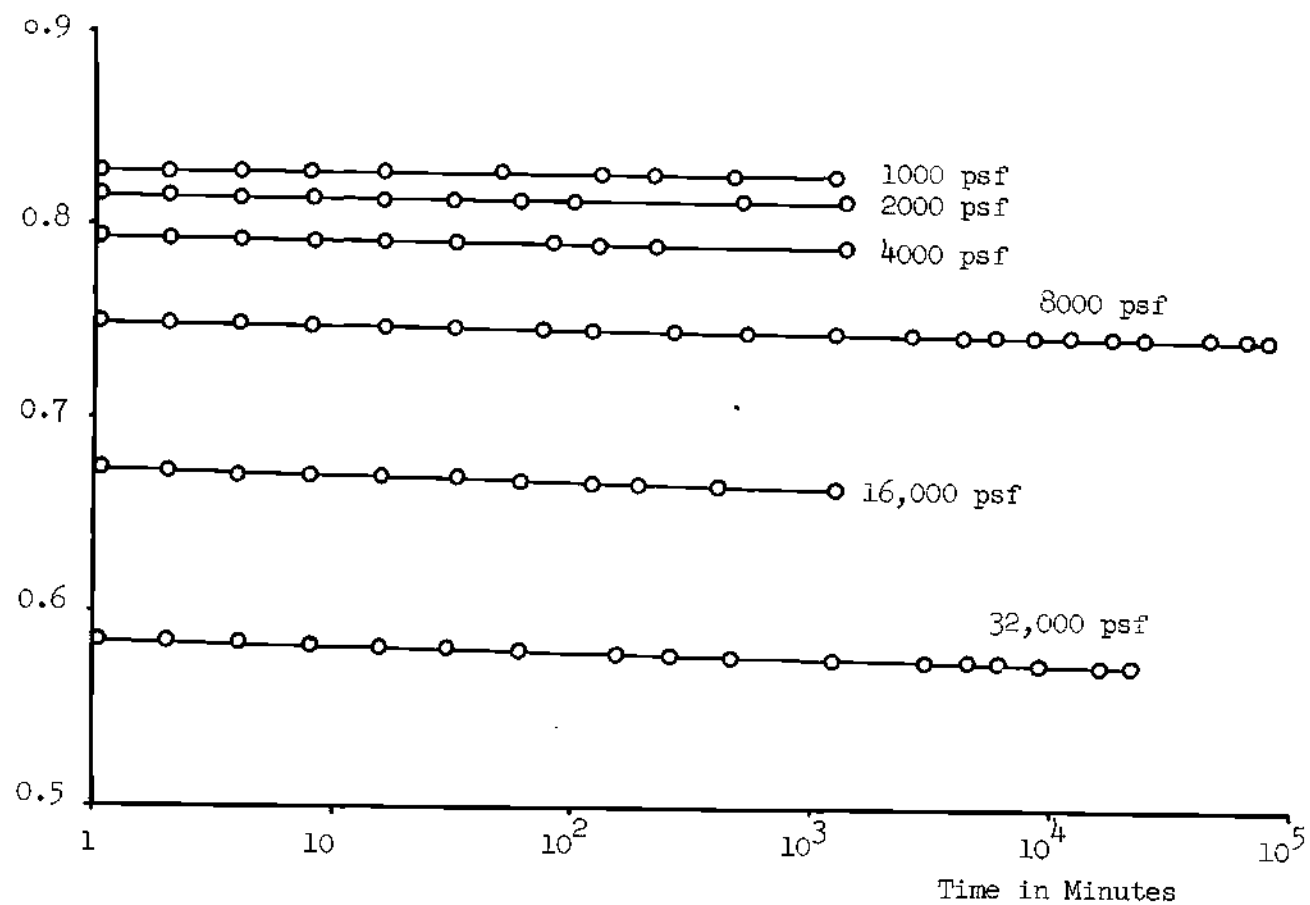


Figure 13. Time-Settlement Curves for Sample U4

Void
Ratio

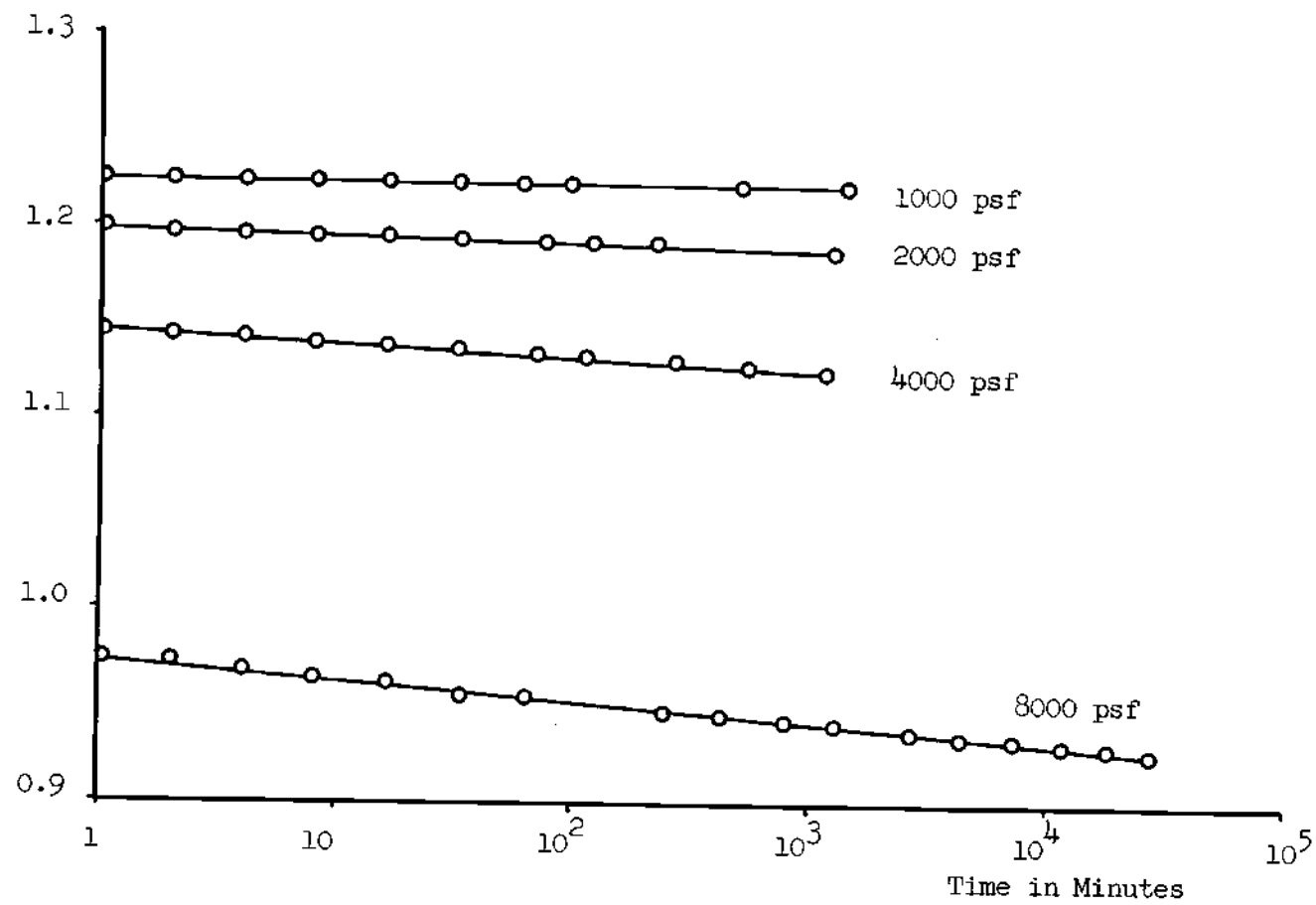


Figure 14. Time-Settlement Curves for Sample U5

Void
Ratio

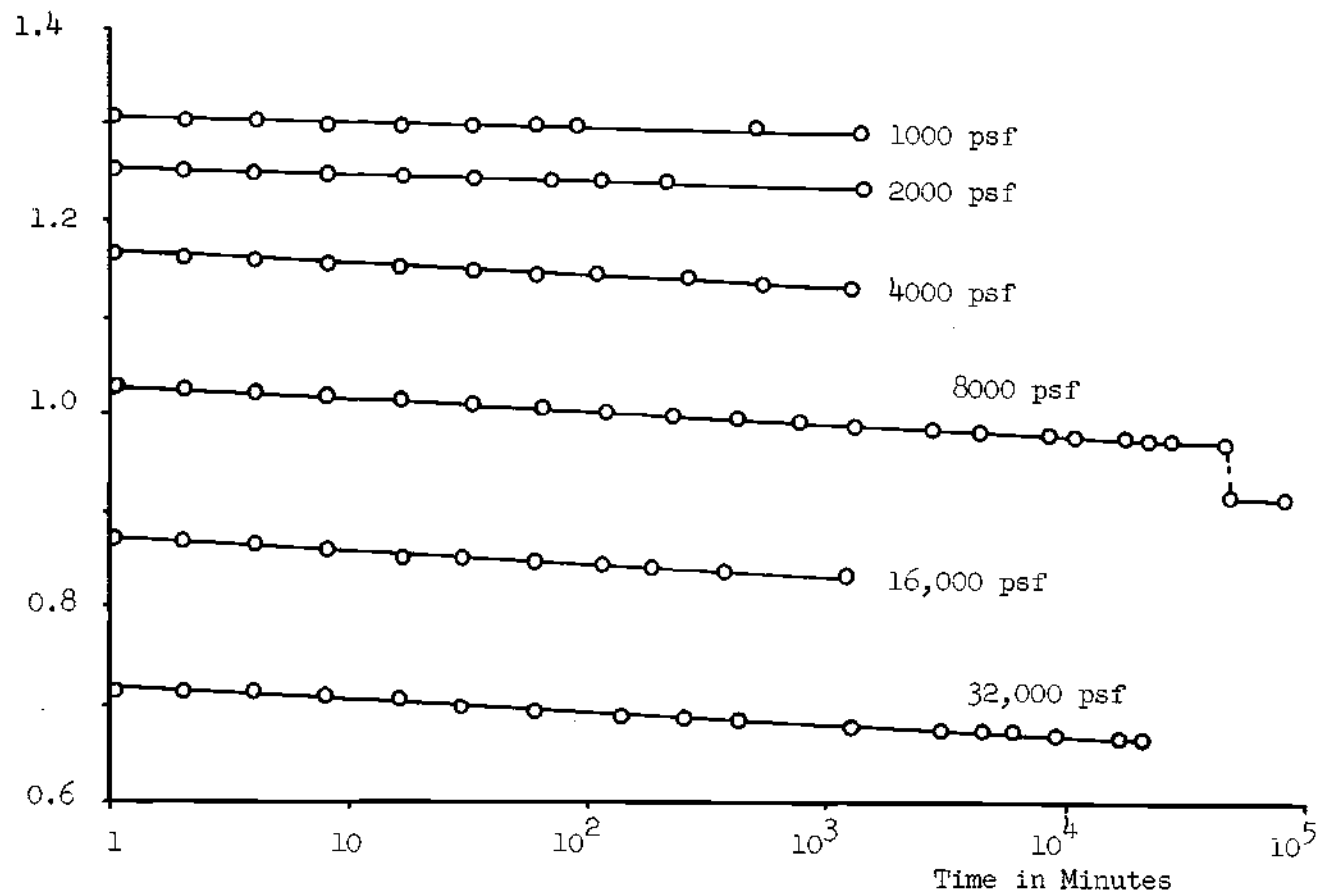


Figure 15. Time-Settlement Curves for Sample U6

Void
Ratio

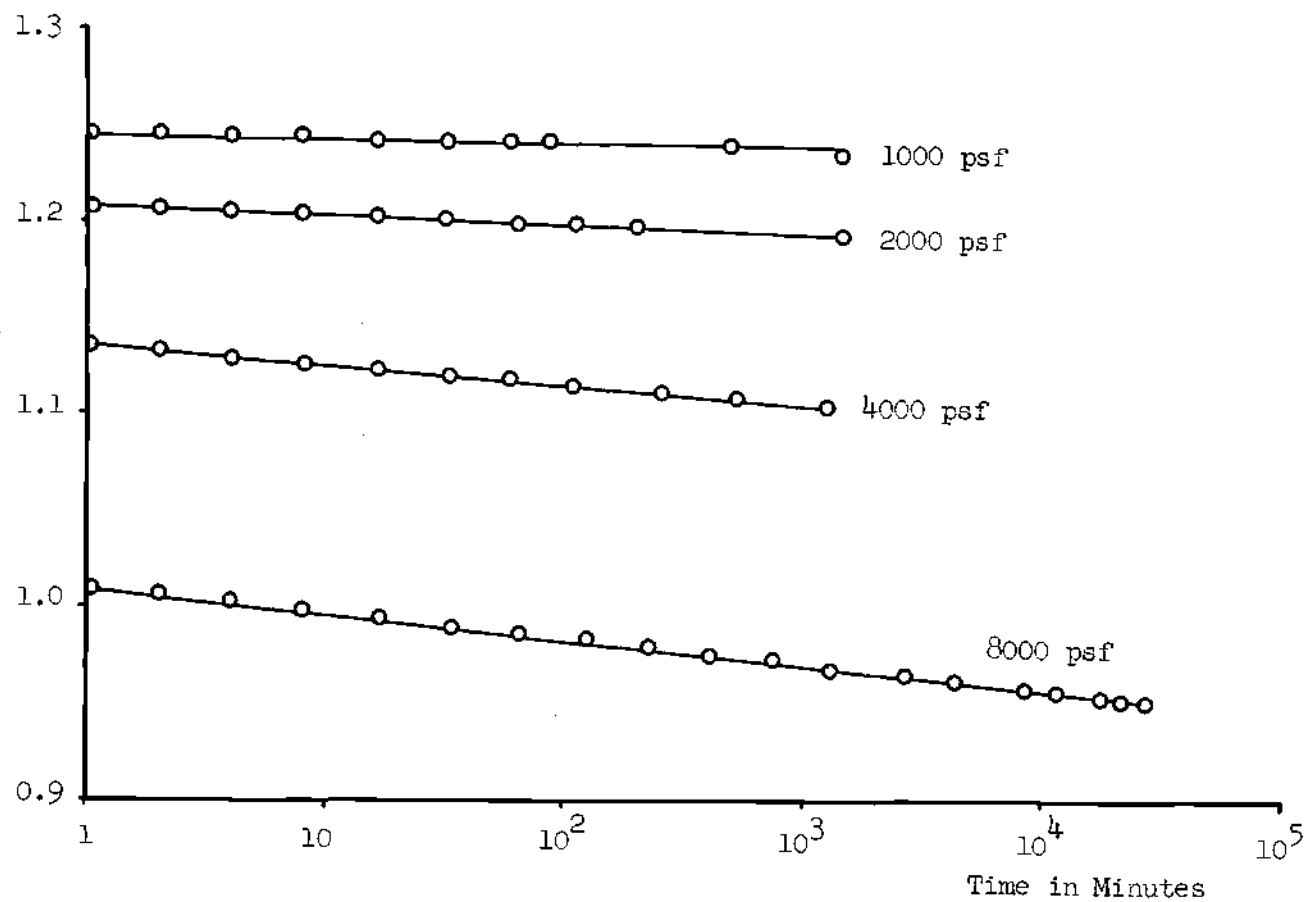


Figure 16. Time-Settlement Curves for Sample U7

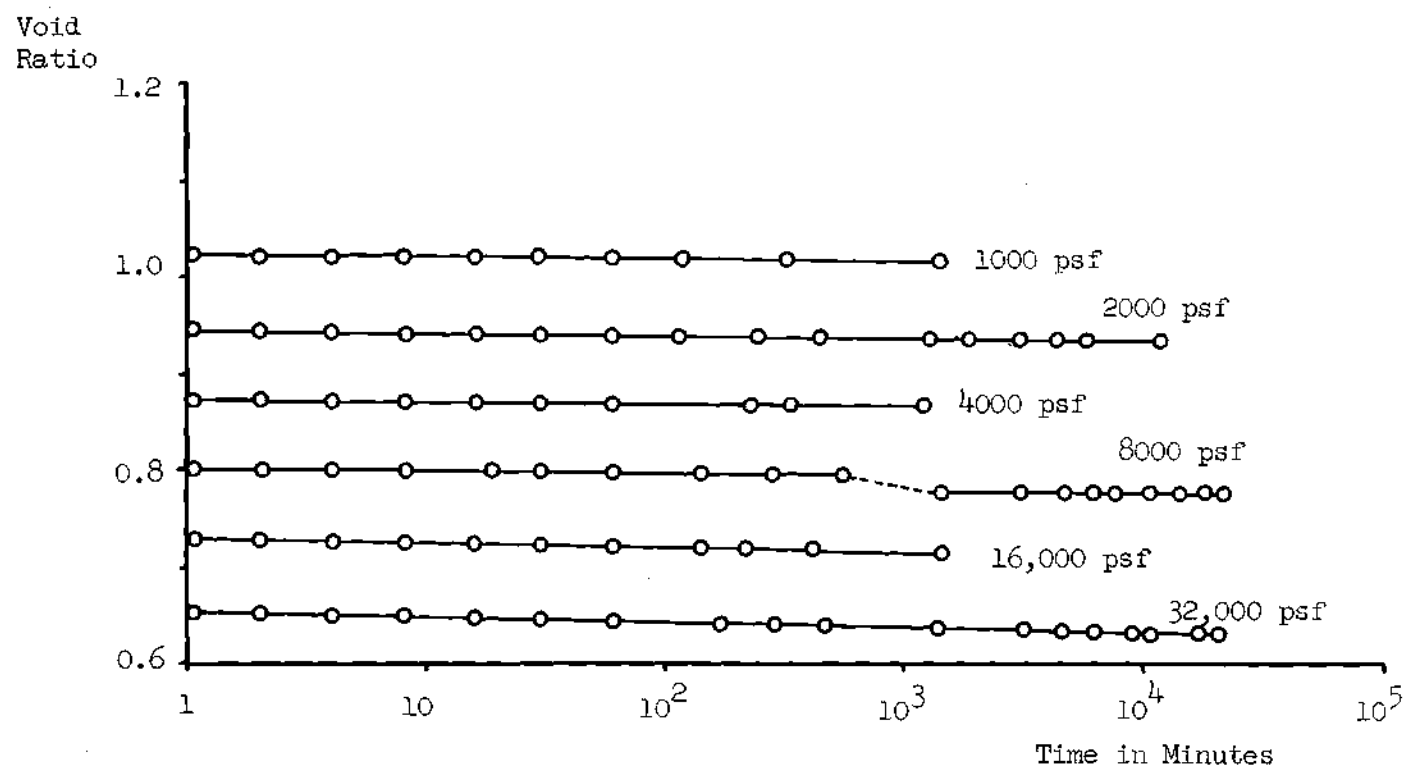


Figure 17. Time-Settlement Curves for Sample R1

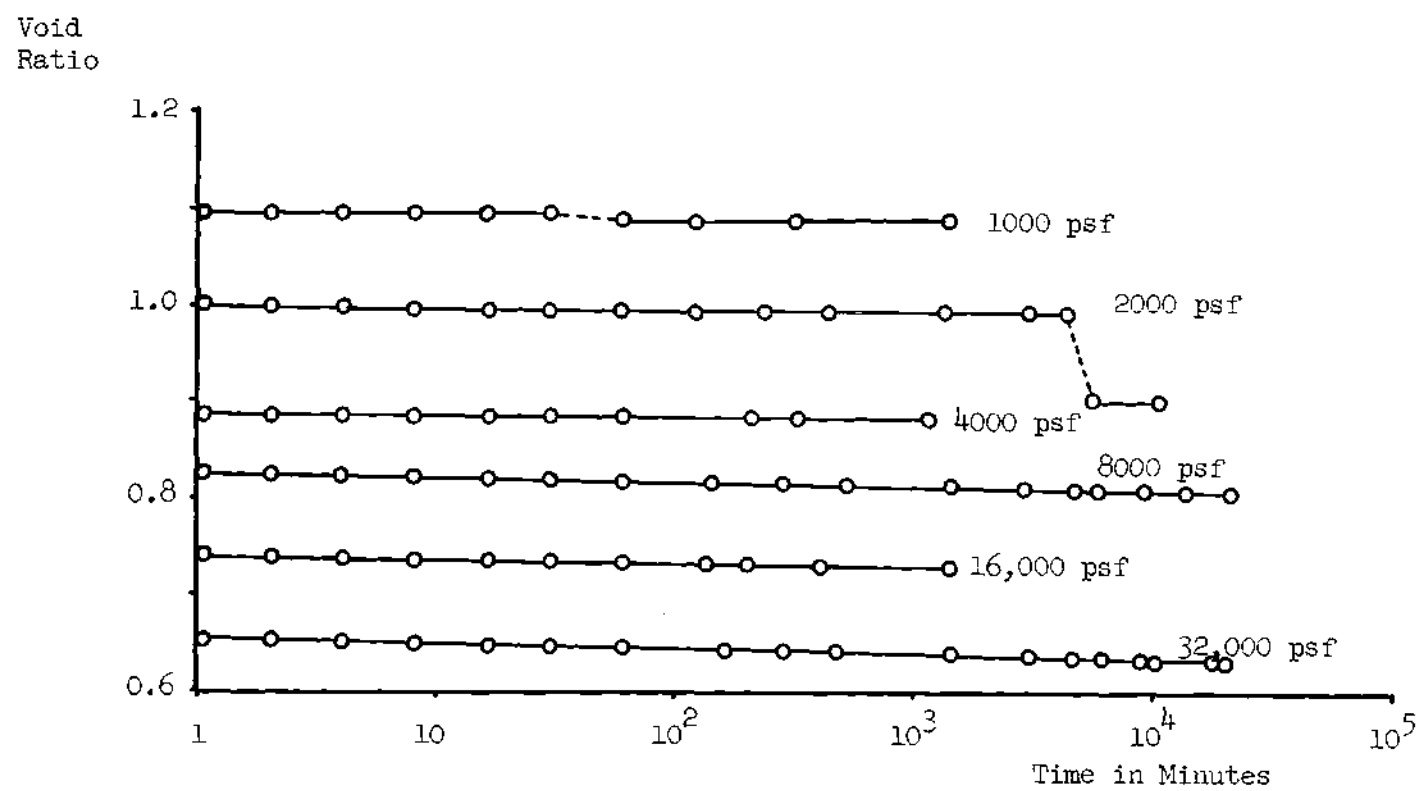


Figure 18. Time-Settlement Curves for Sample R2

Void
Ratio

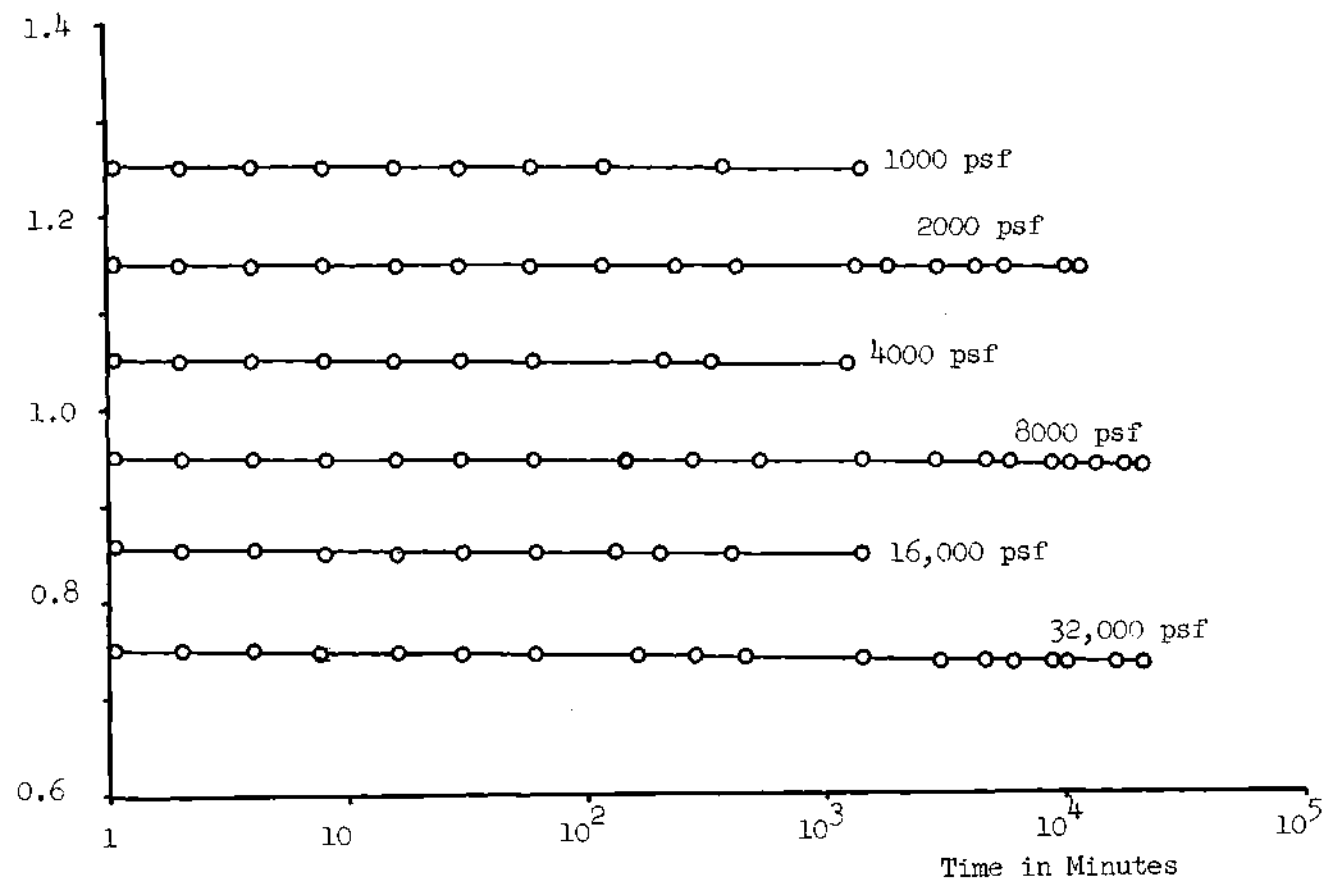


Figure 19. Time-Settlement Curves for Sample R3

Void
Ratio

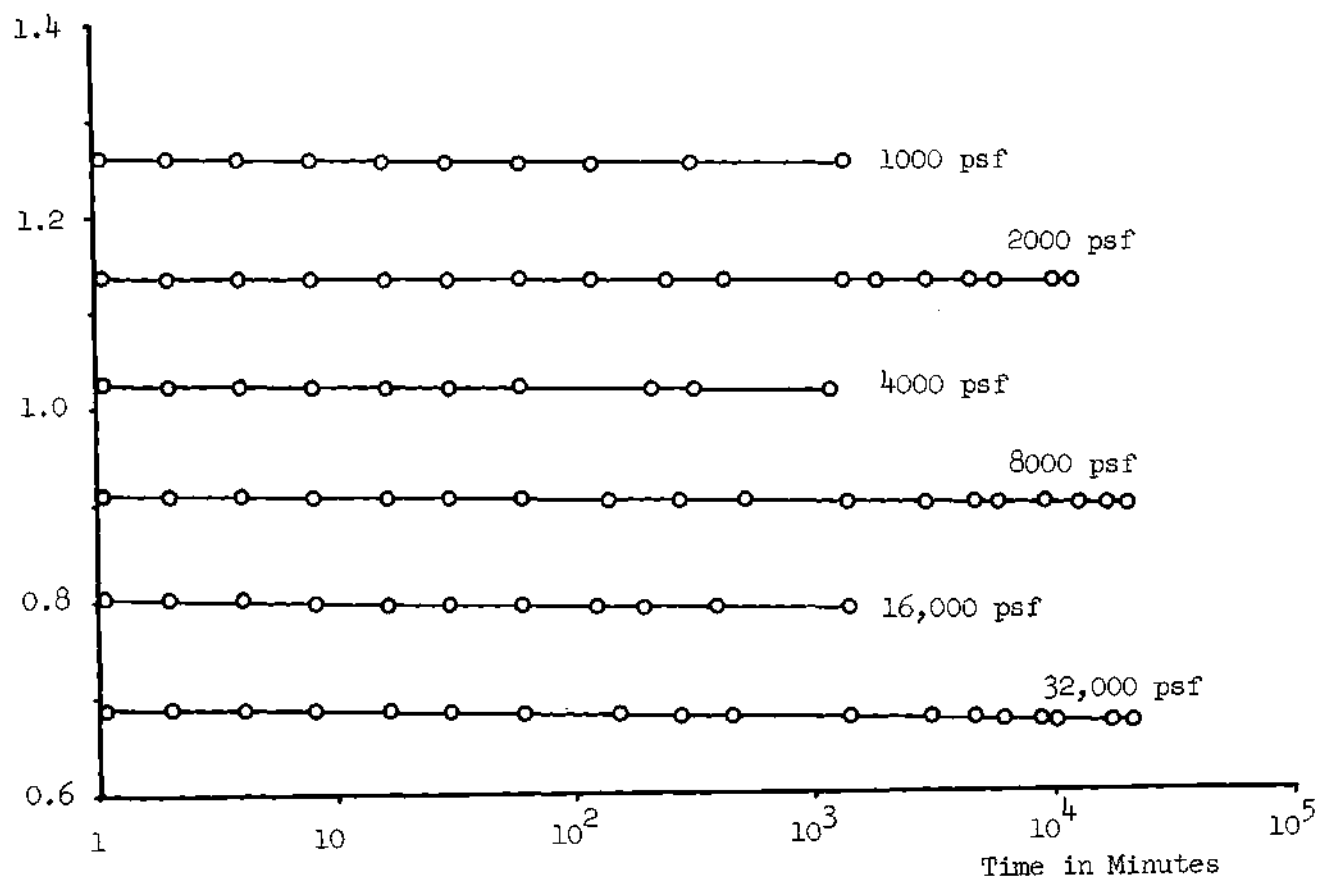


Figure 20. Time-Settlement Curves for Sample R4

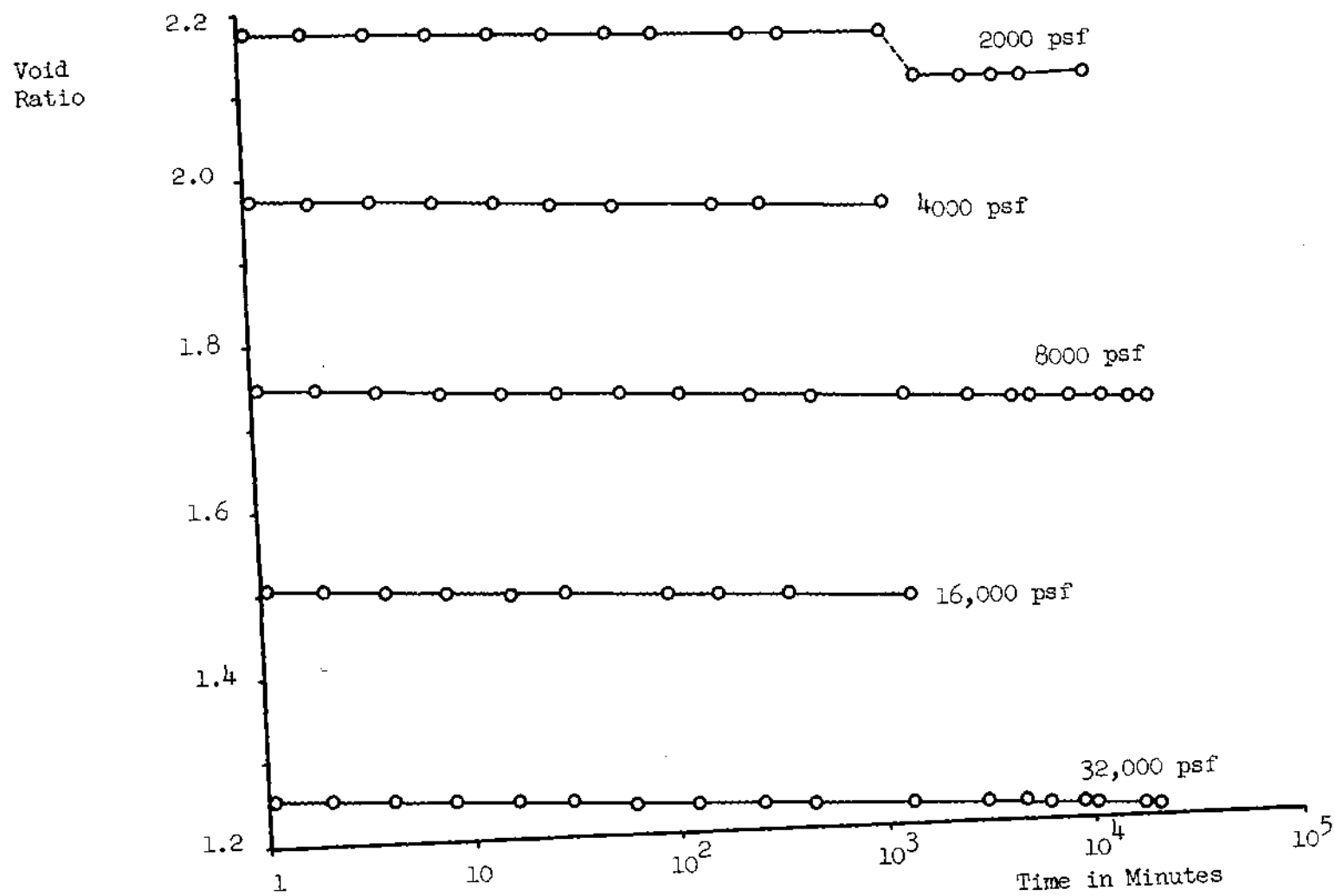


Figure 21. Time-Settlement Curves for Sample R5

Void
Ratio

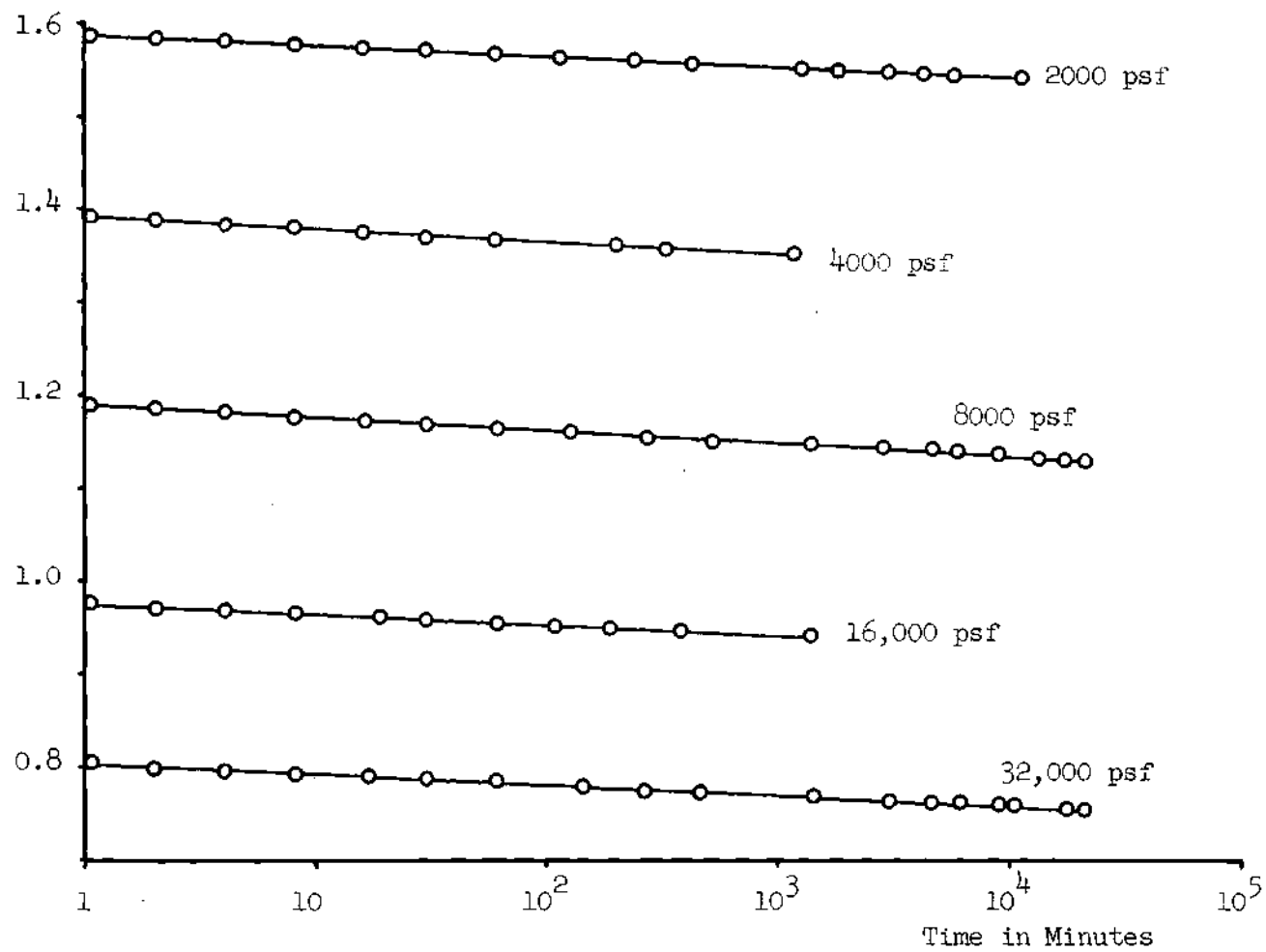


Figure 22. Time-Settlement Curves for Sample R6

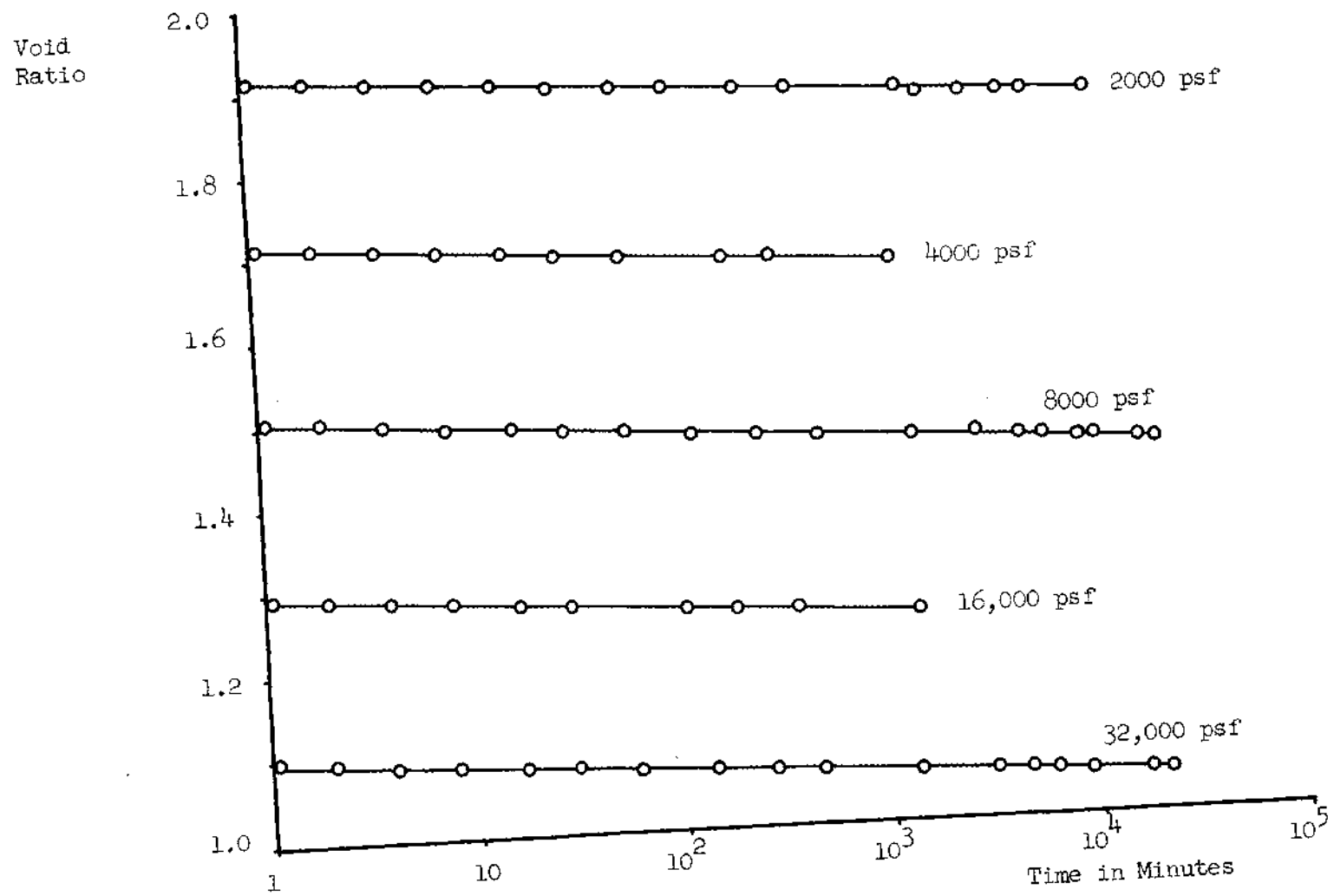


Figure 23. Time-Settlement Curves for Sample R7

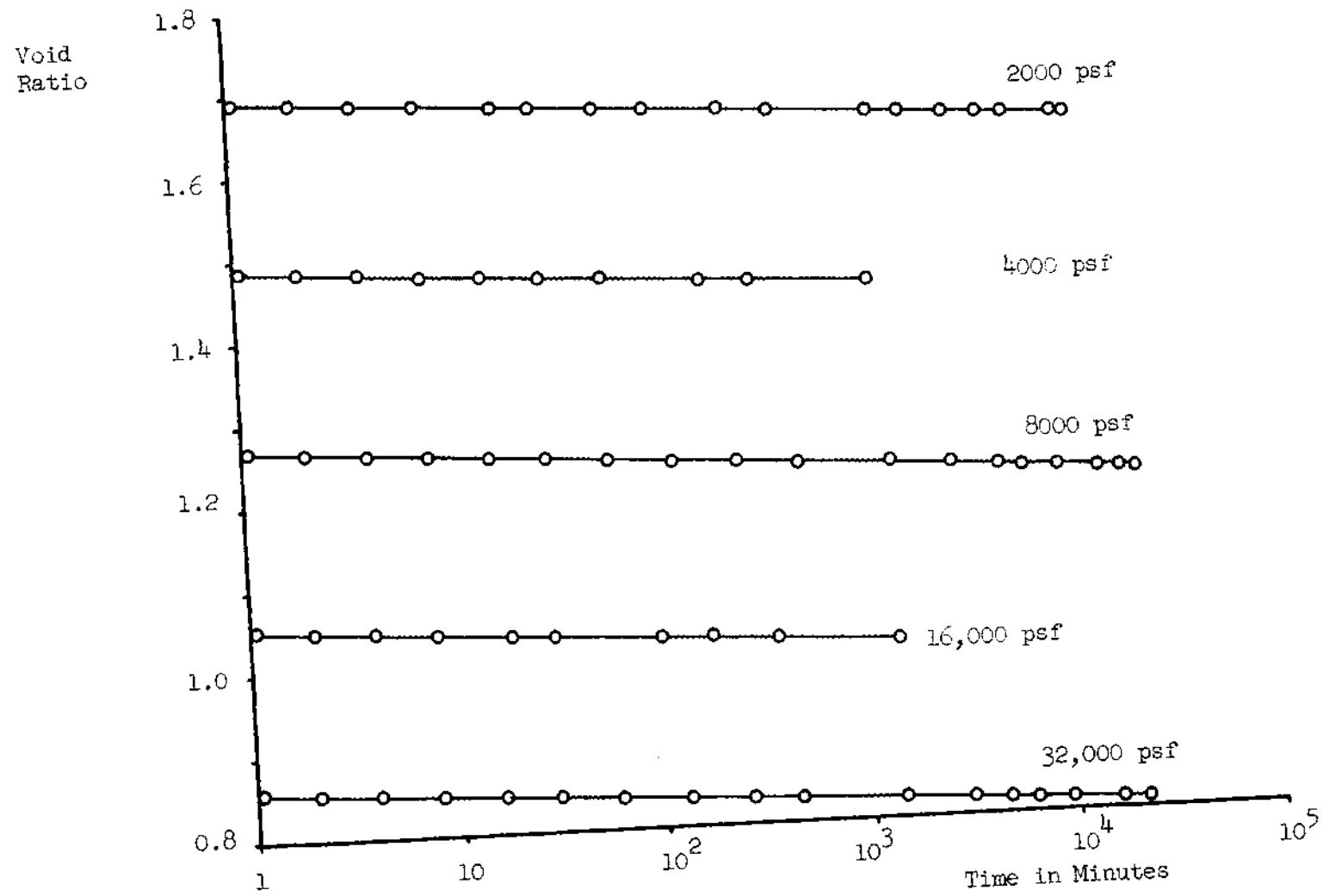


Figure 24. Time-Settlement Curves for Sample R8

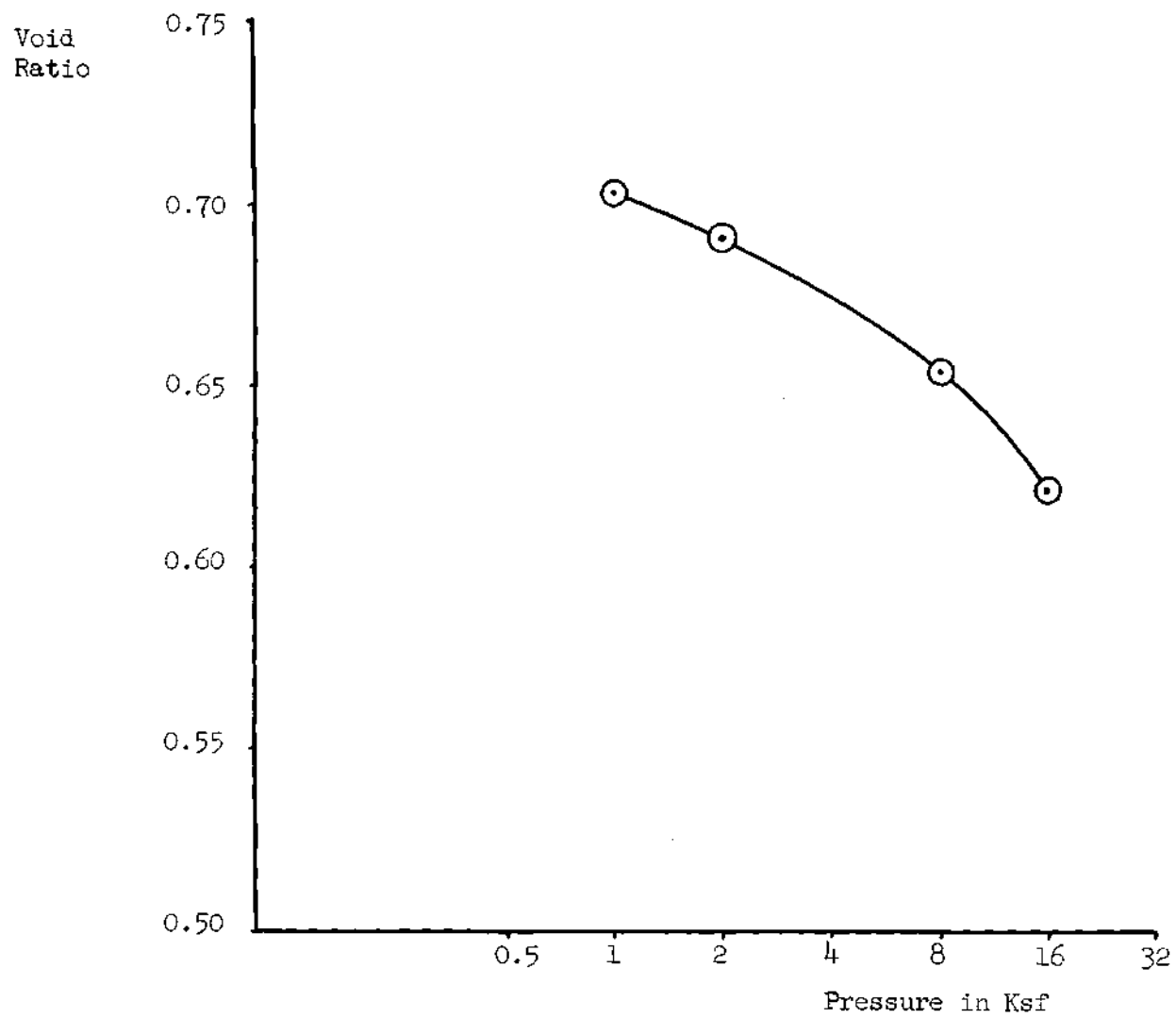


Figure 25. Pressure Settlement Curve for Sample U1

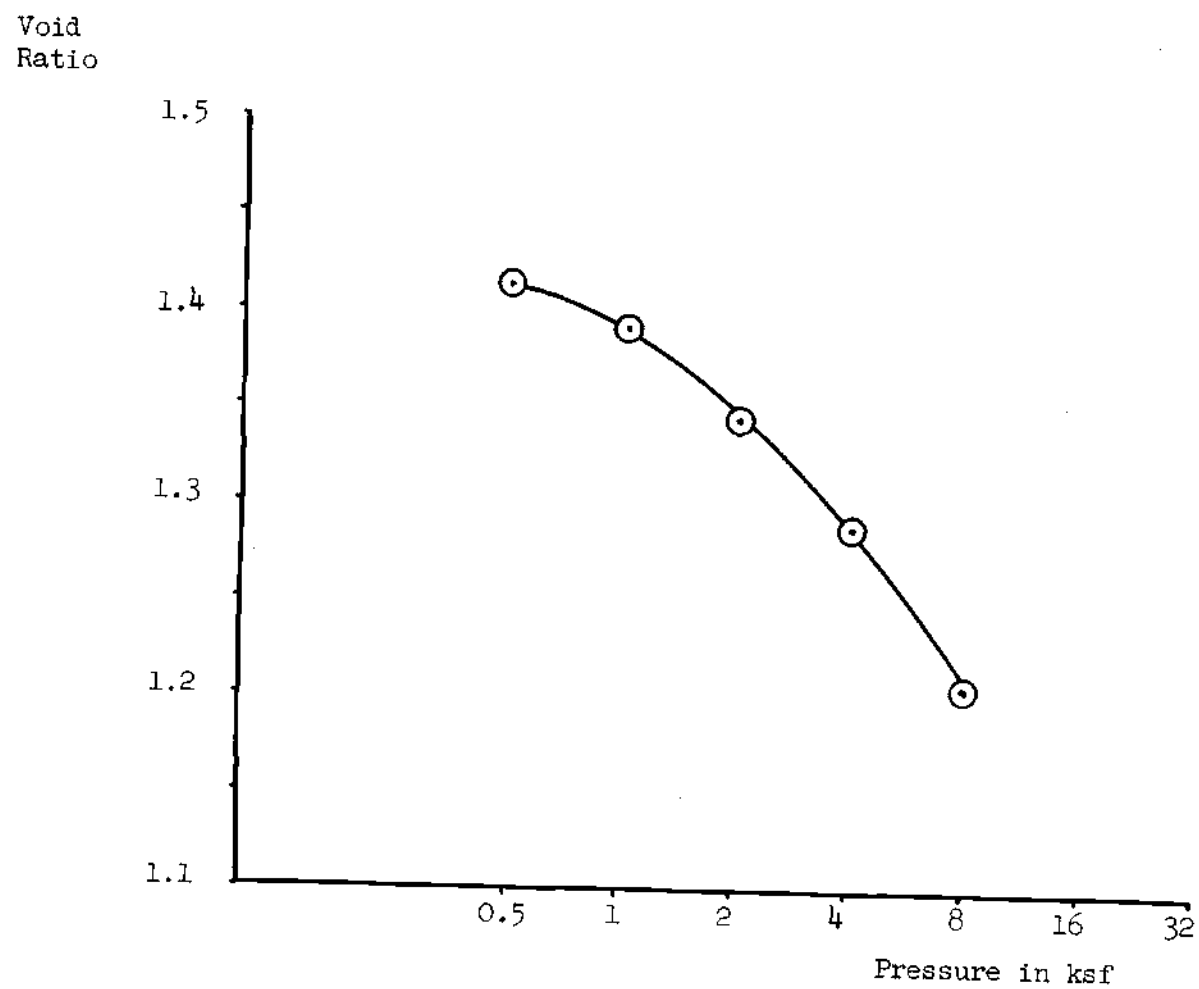


Figure 26. Pressure-Settlement Curve for Sample U2

Void
Ratio

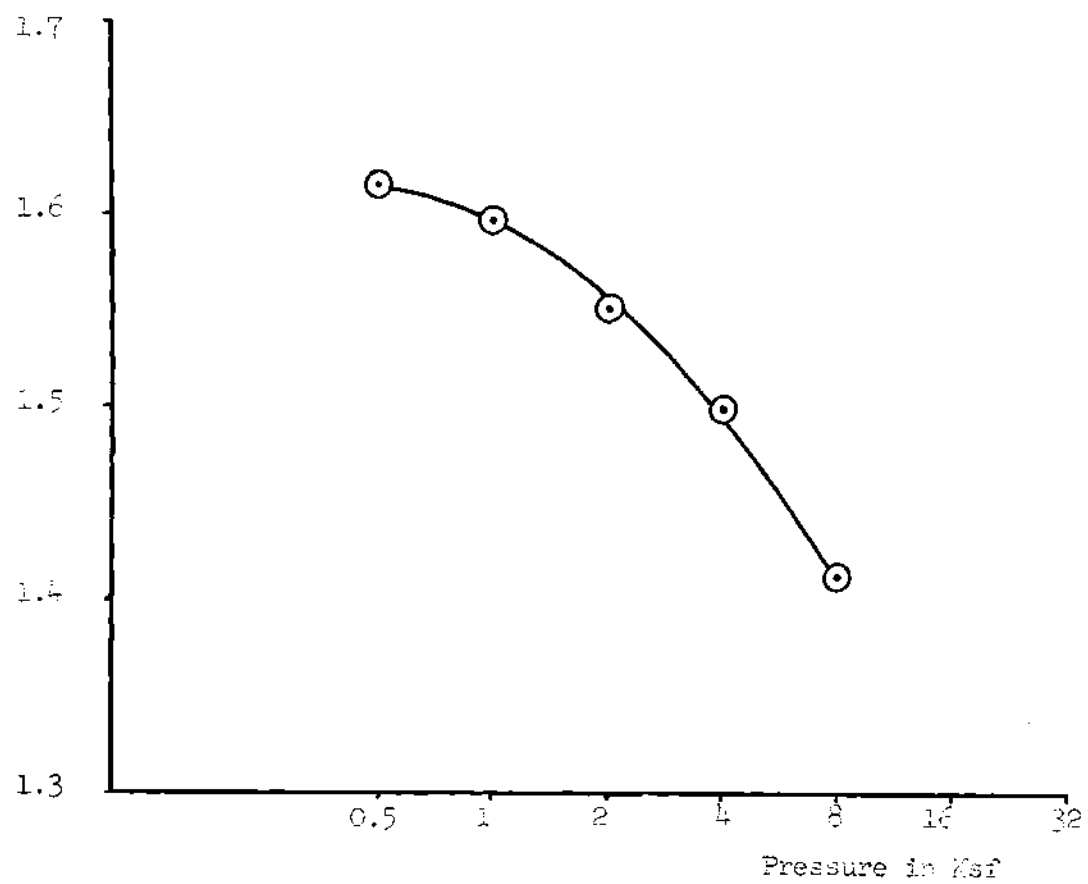


Figure 27. Pressure-Settlement Curve for Sample U3

Void
Ratio

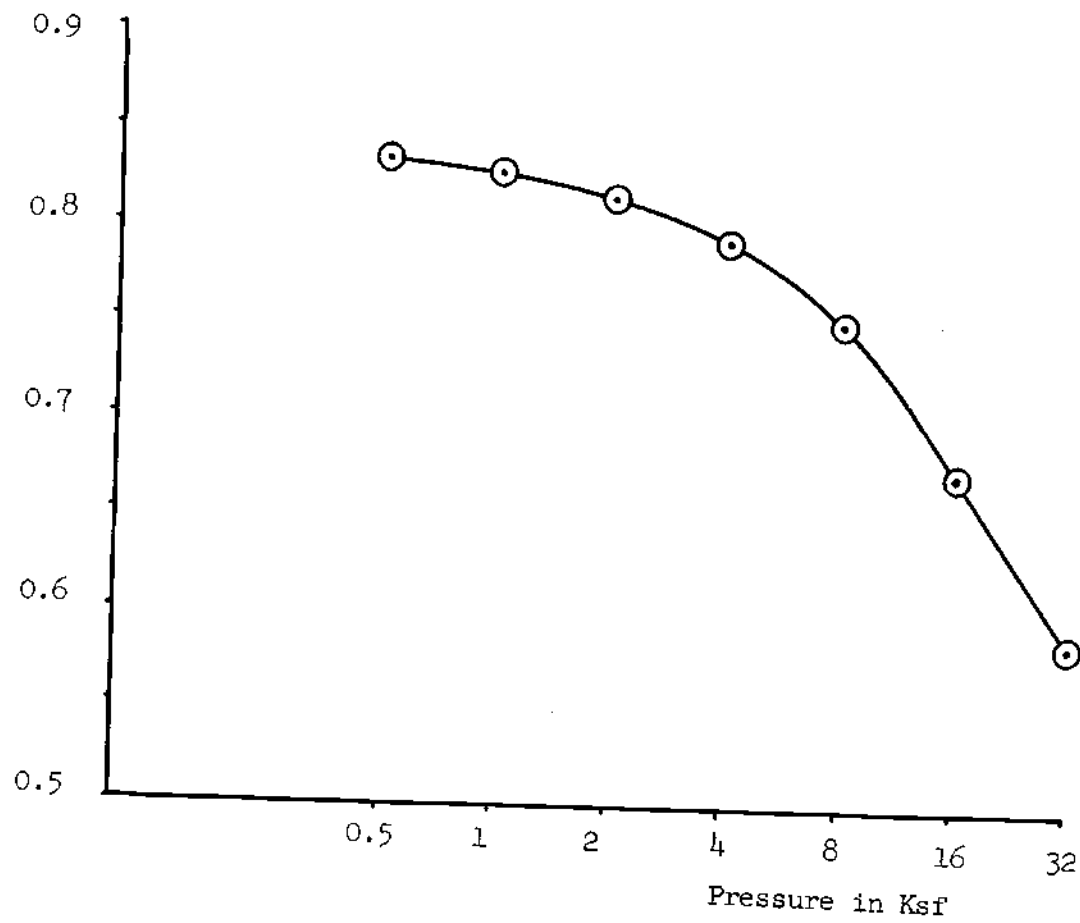


Figure 28. Pressure-Settlement Curve for Sample U4

Void
Ratio

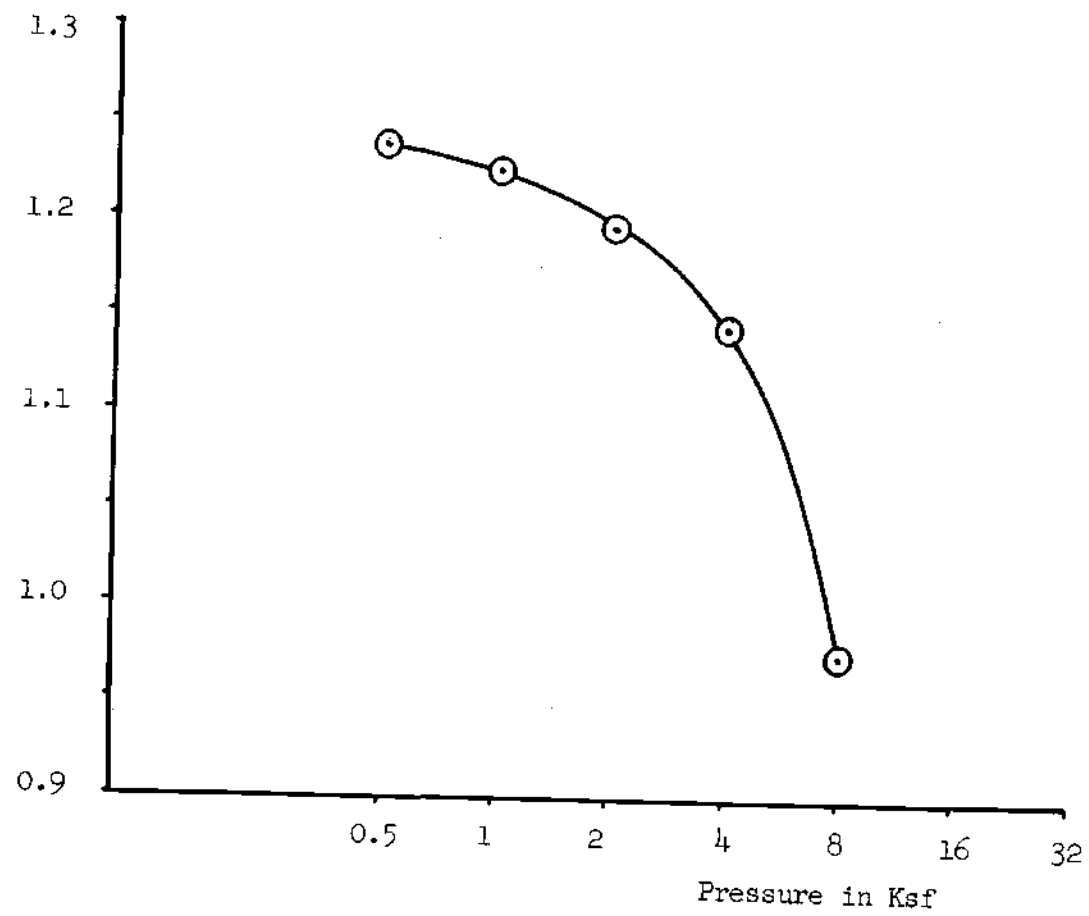


Figure 29. Pressure-Settlement Curve for Sample U5

Void
Ratio

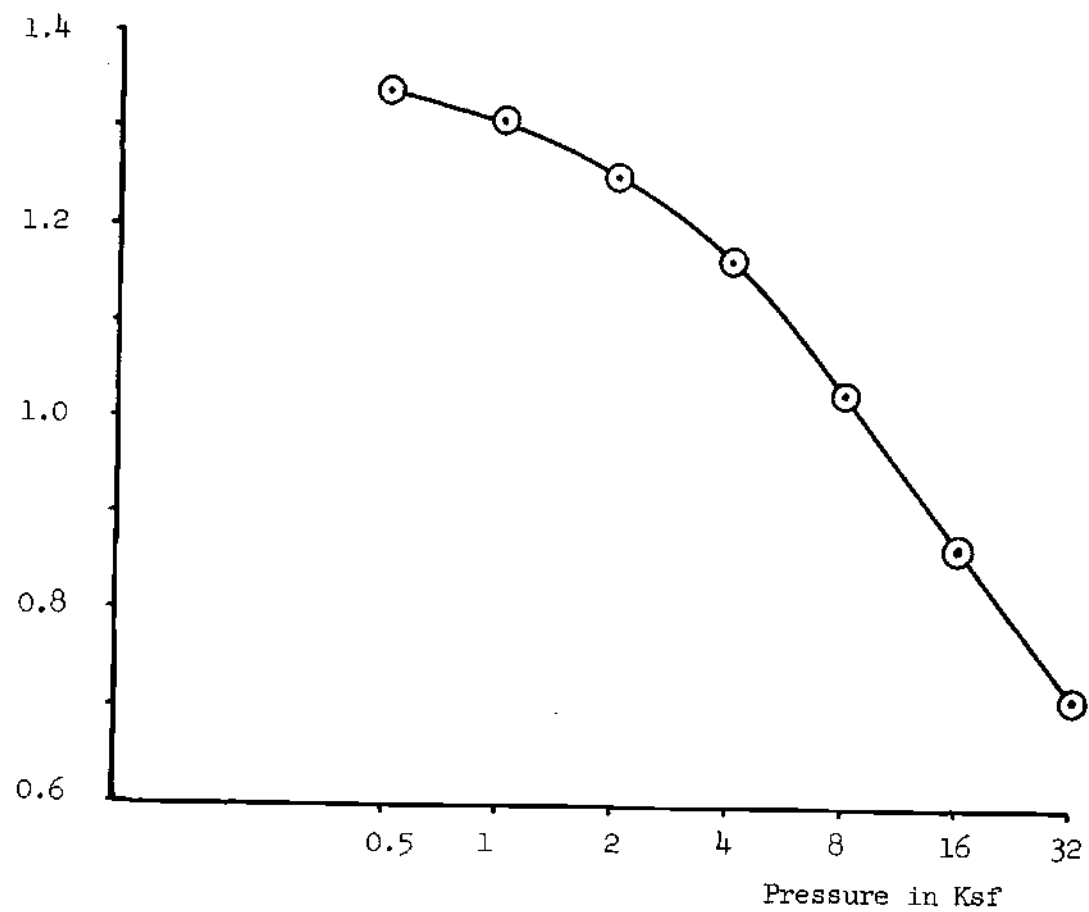


Figure 30. Pressure-Settlement Curve for Sample U6

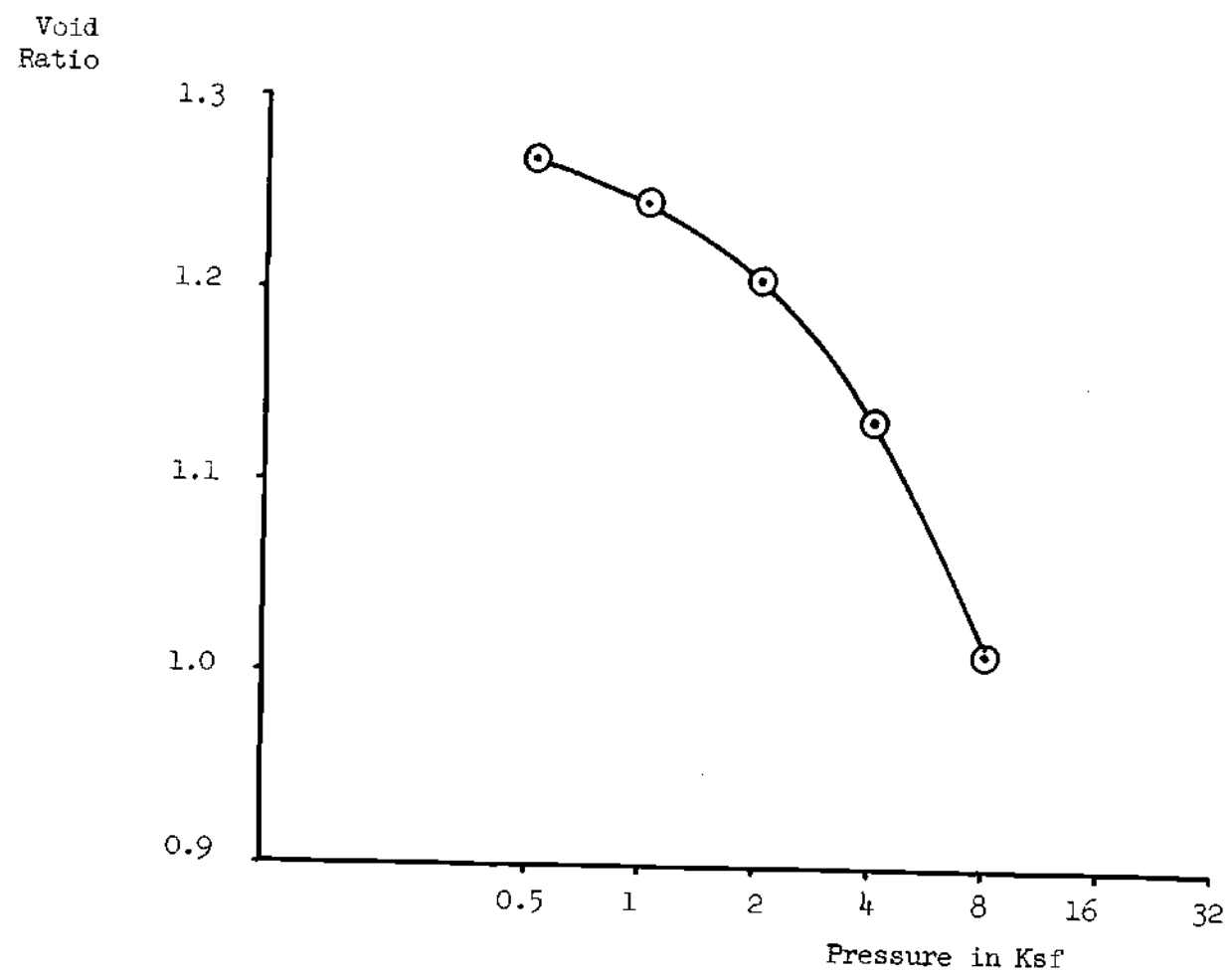


Figure 31. Pressure-Settlement Curve for Sample U7

Void
Ratio

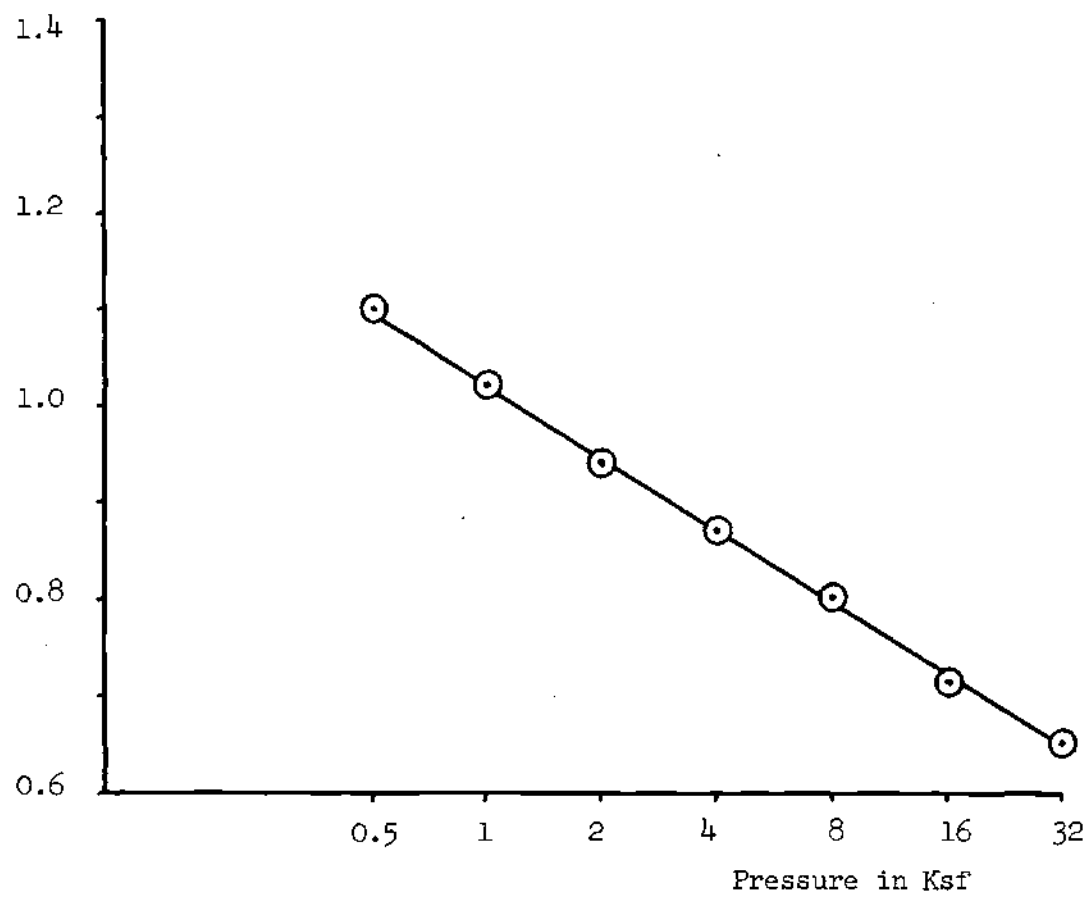


Figure 32. Pressure-Settlement Curve for Sample R1

Void
Ratio

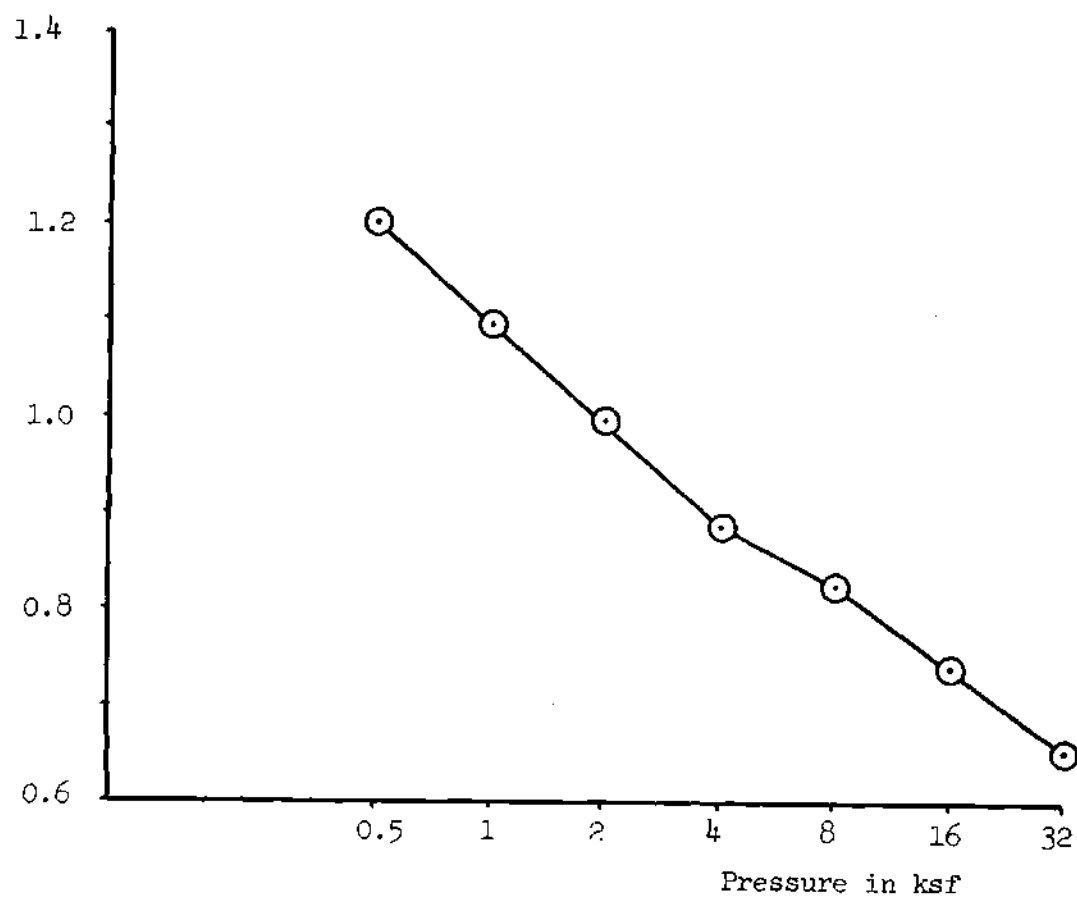


Figure 33. Pressure-Settlement Curve for Sample R2

Void
Ratio

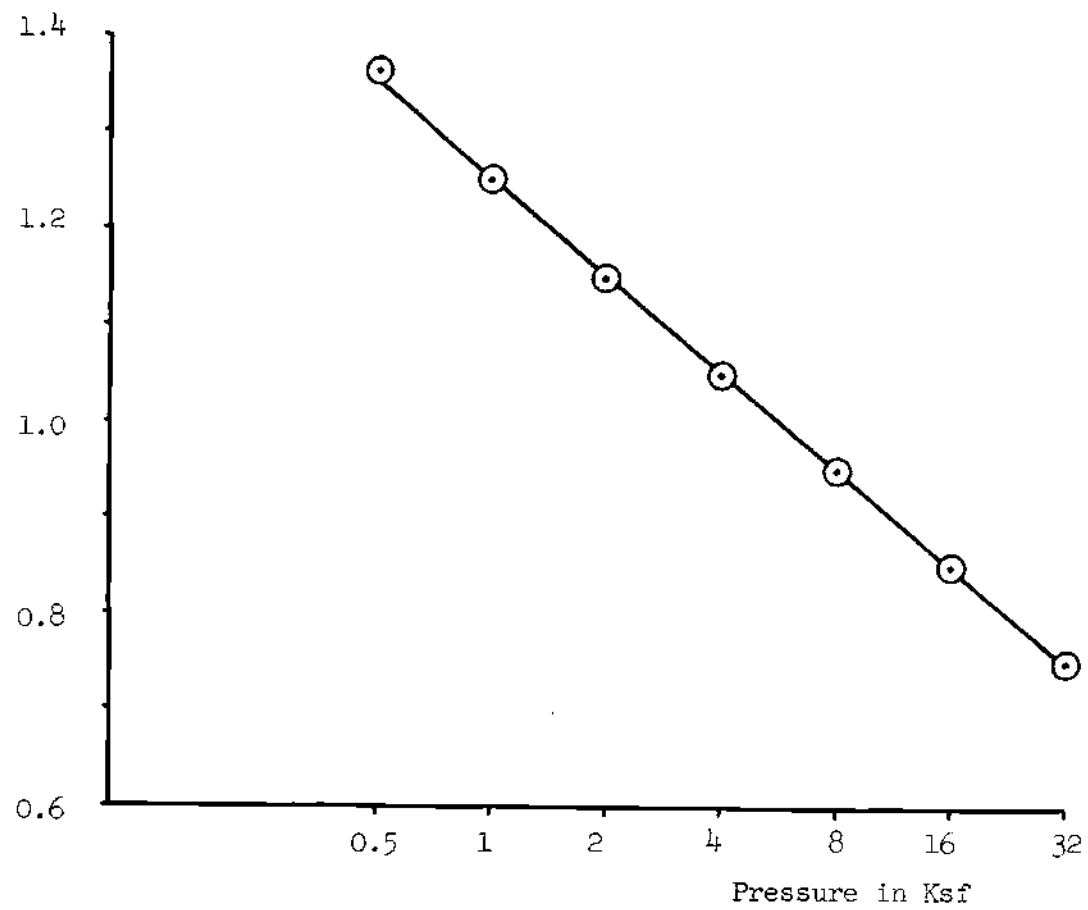


Figure 34. Pressure-Settlement Curve for Sample R3

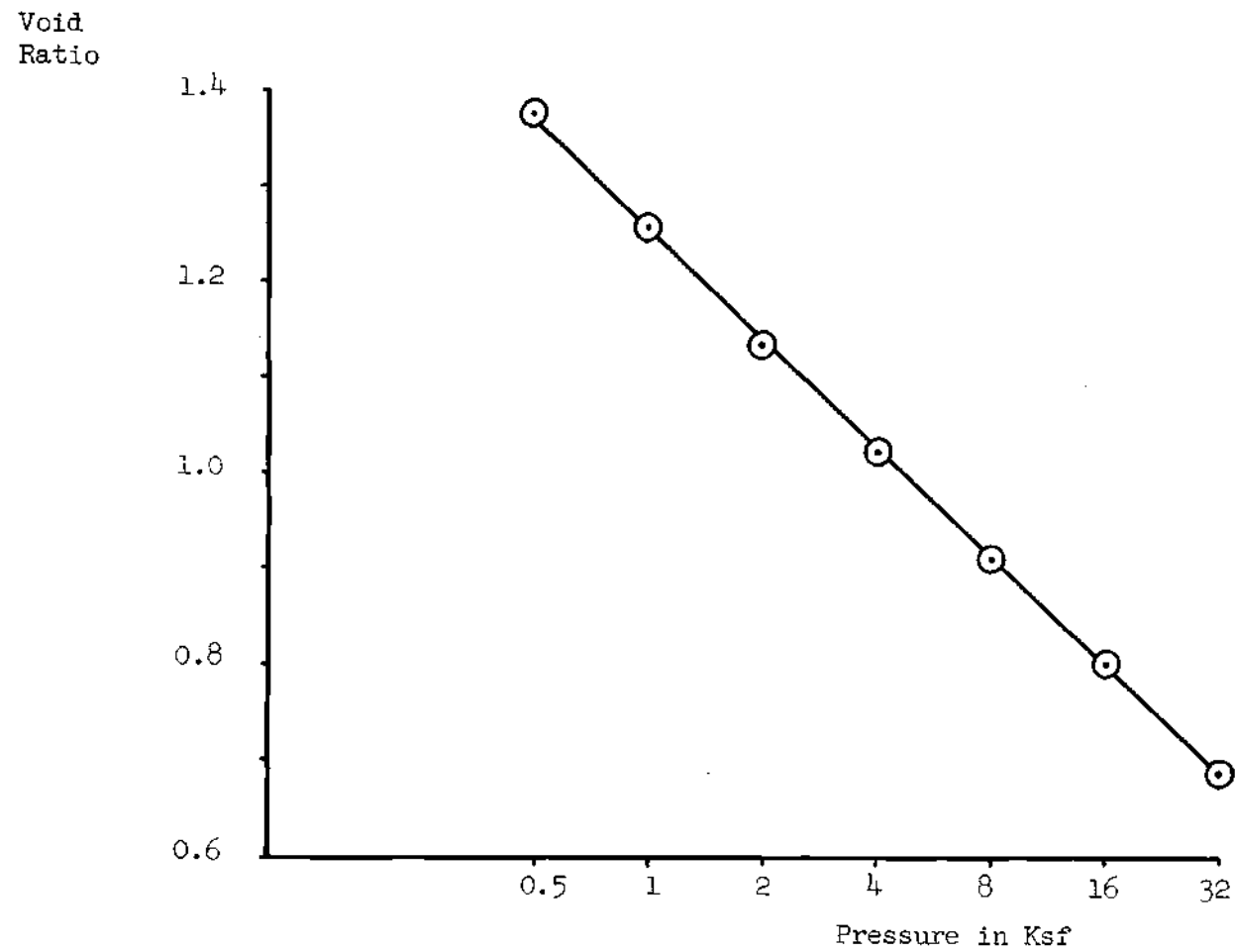


Figure 35. Pressure-Settlement Curve for Sample R4

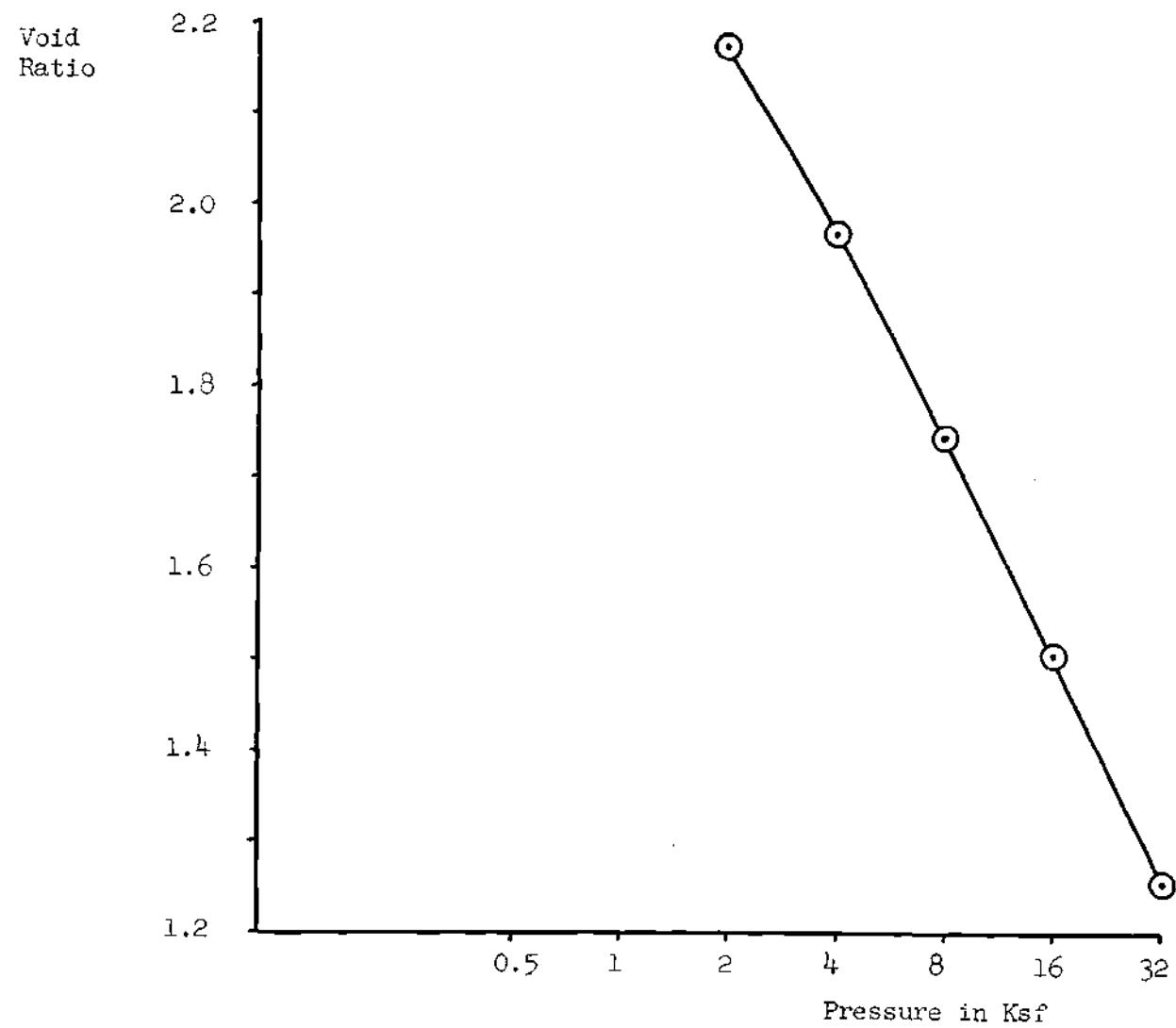


Figure 36. Pressure-Settlement Curve for Sample R5

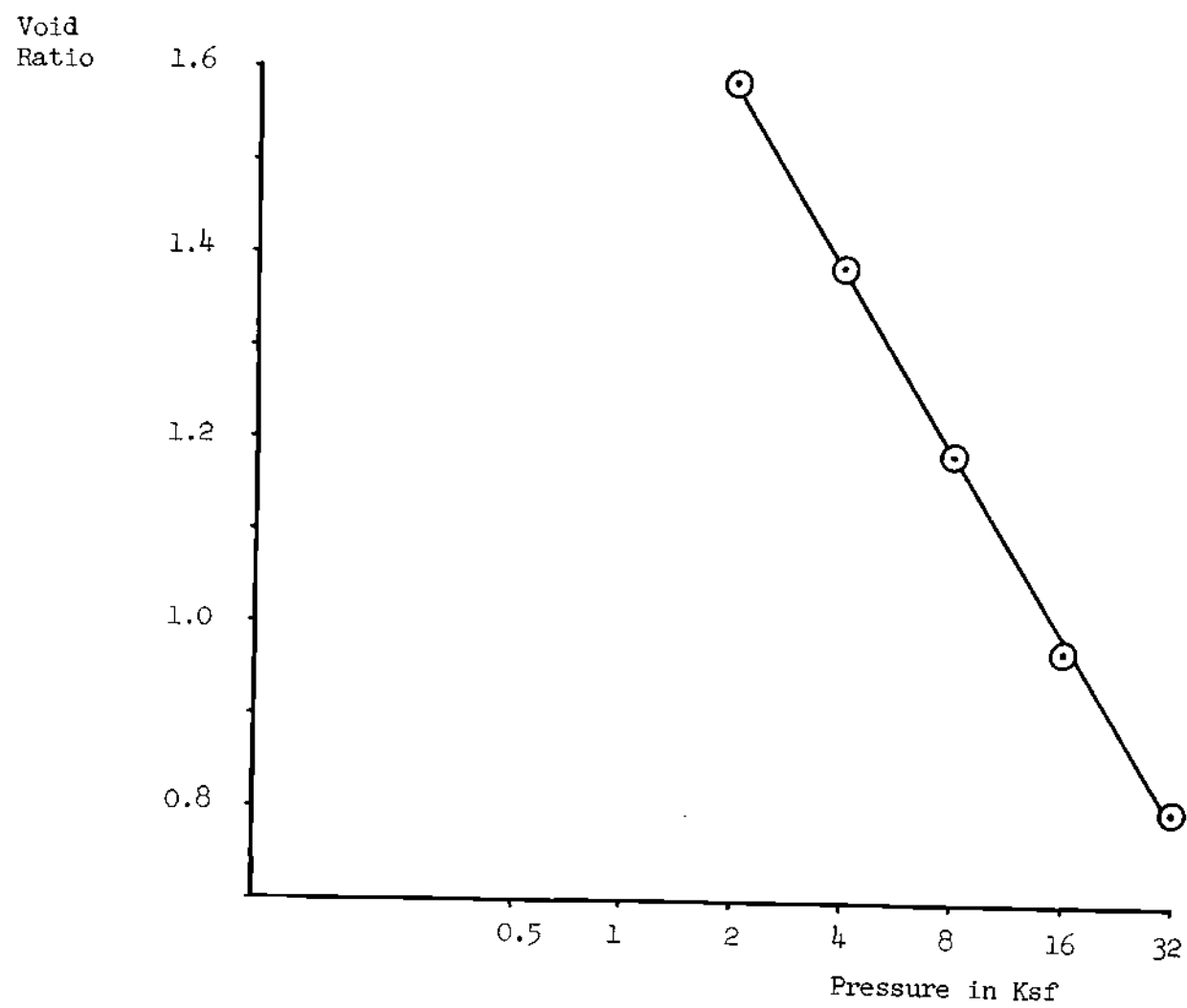


Figure 37. Pressure-Settlement Curve for Sample R6

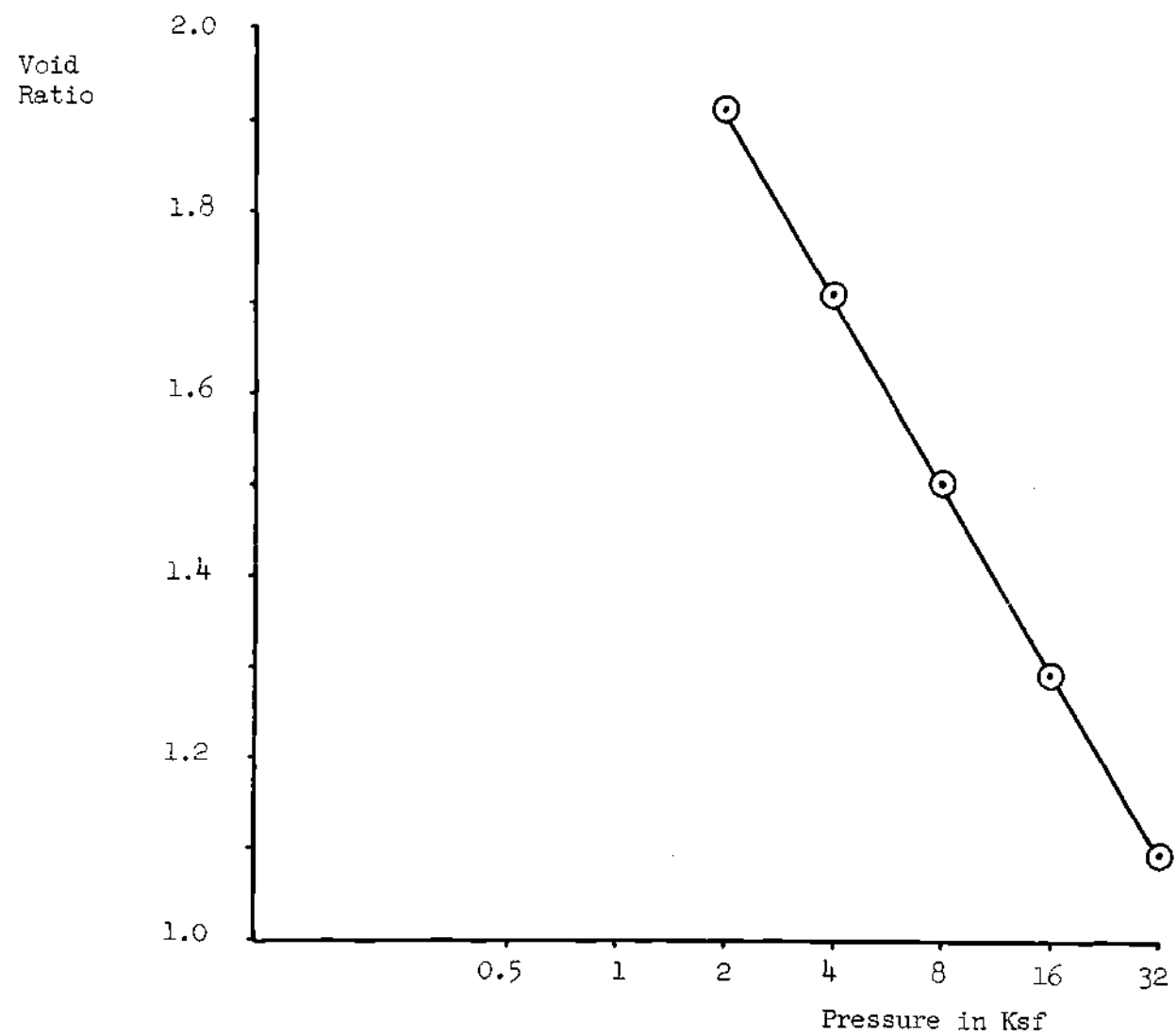


Figure 38. Pressure-Settlement Curve for Sample R7

Void
Ratio

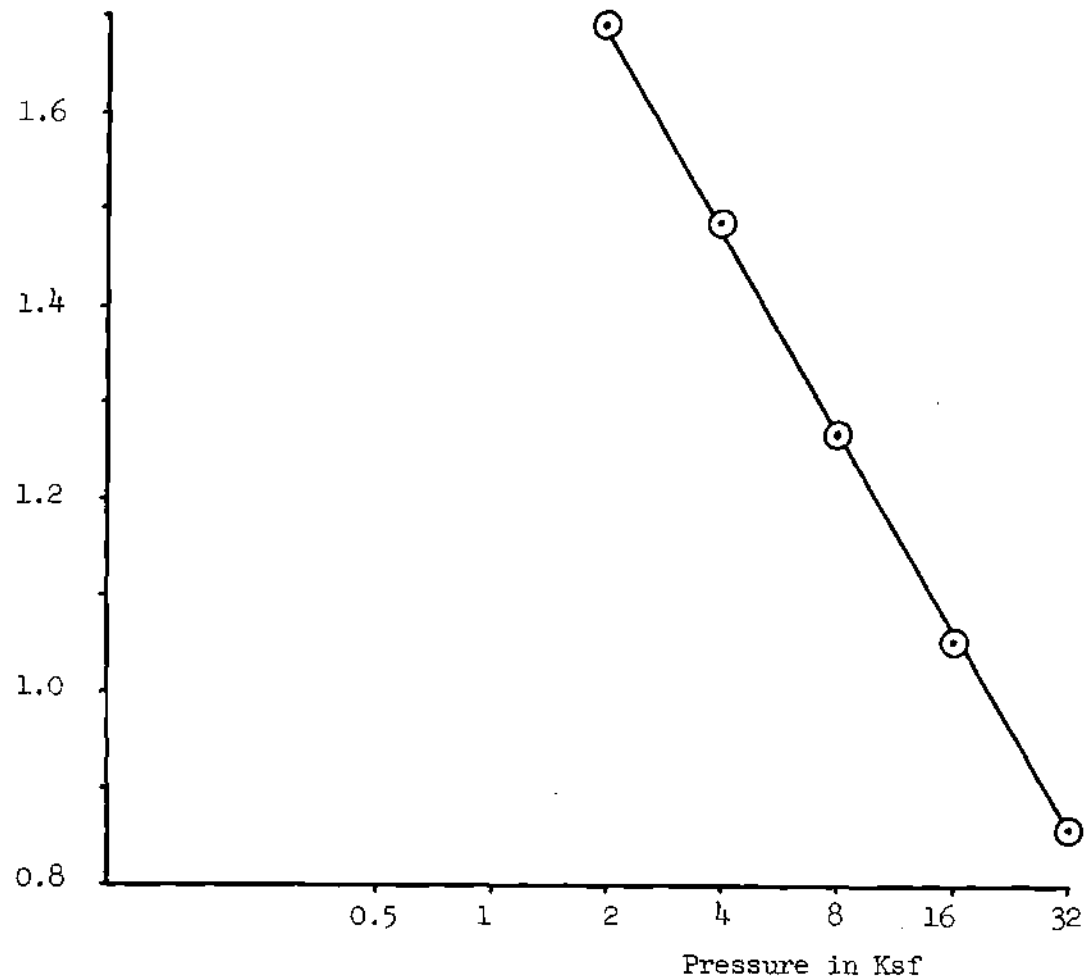


Figure 39. Pressure-Settlement Curve for Sample R8

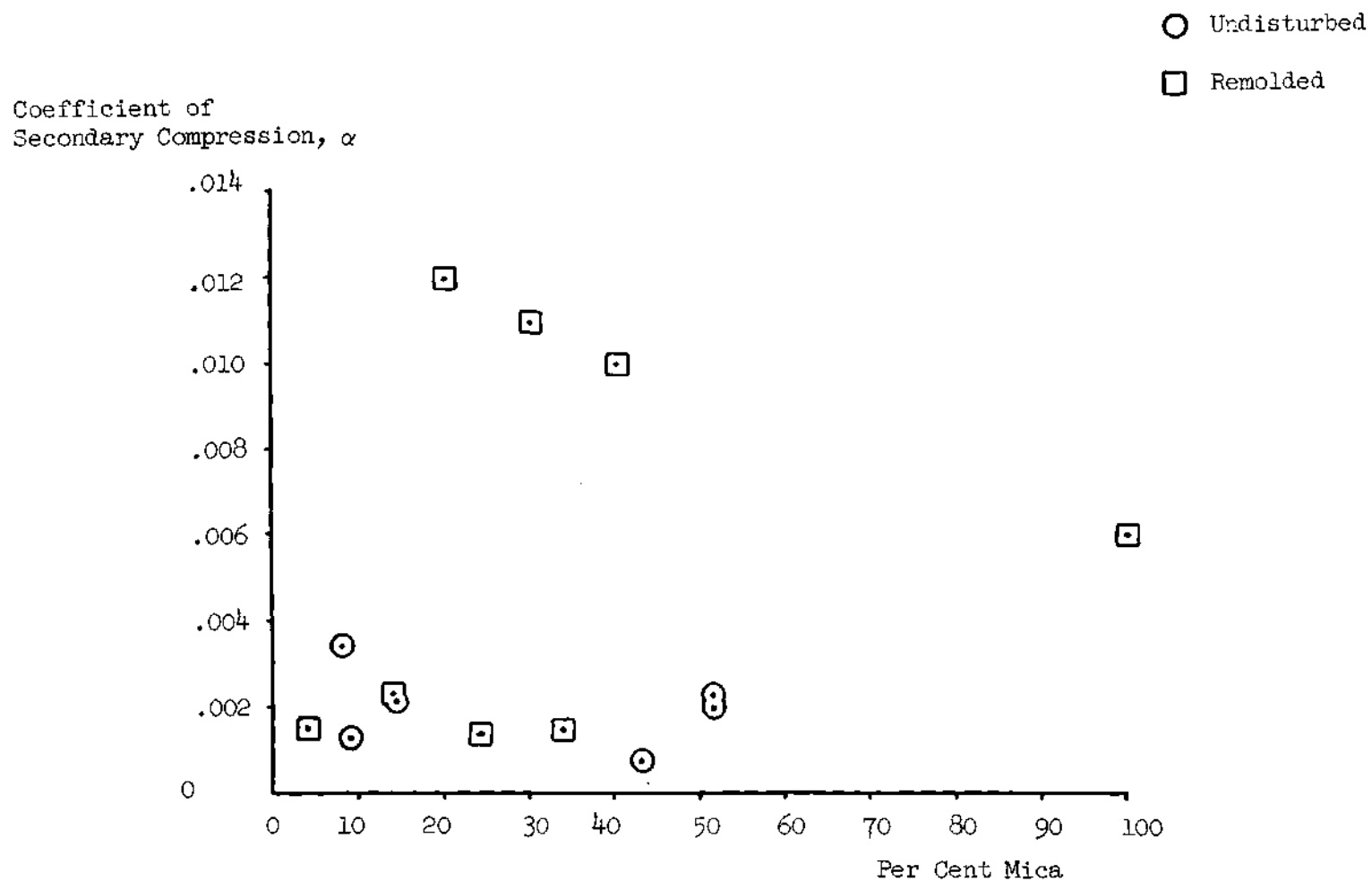


Figure 40. Relationship Between Mica Content and the Coefficient of Secondary Compression under 1000 psf

Coefficient of
Secondary Compression, α

○ Undisturbed

□ Remolded

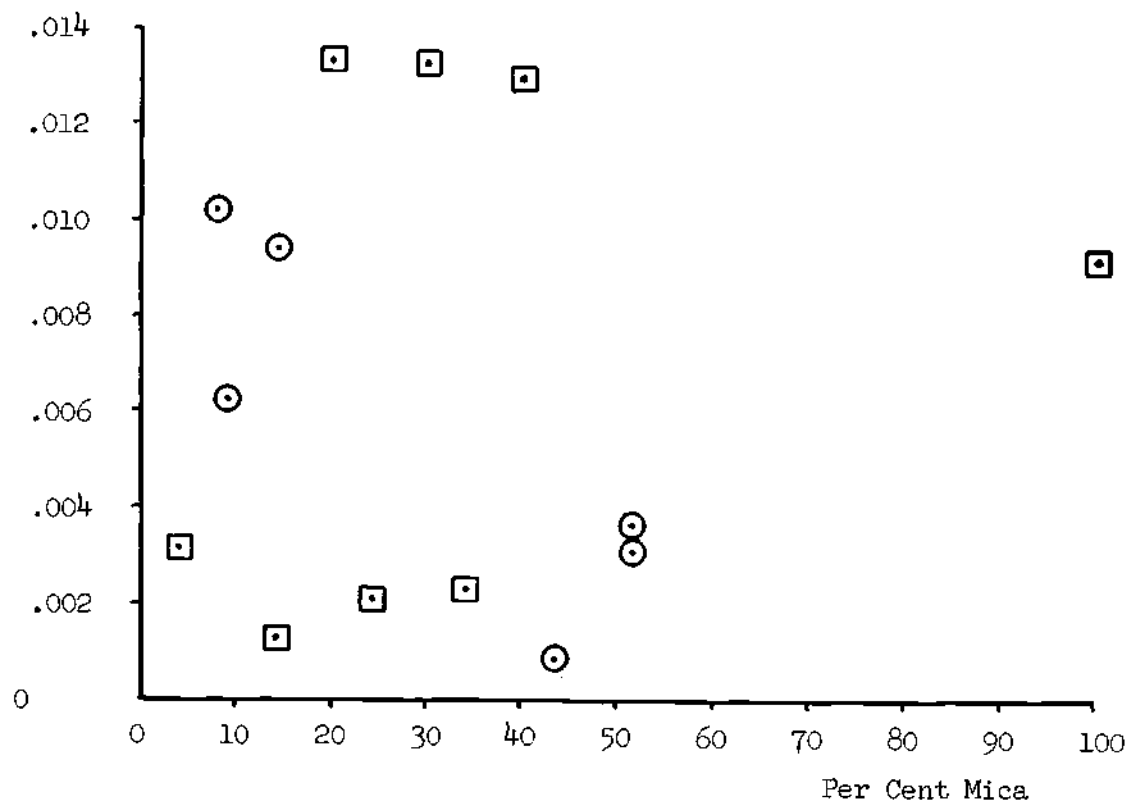


Figure 41. Relationship between Mica Content and the Coefficient of Secondary Compression under 4000 psf

Coefficient of
Secondary Compression, α

○ Undisturbed

□ Remolded

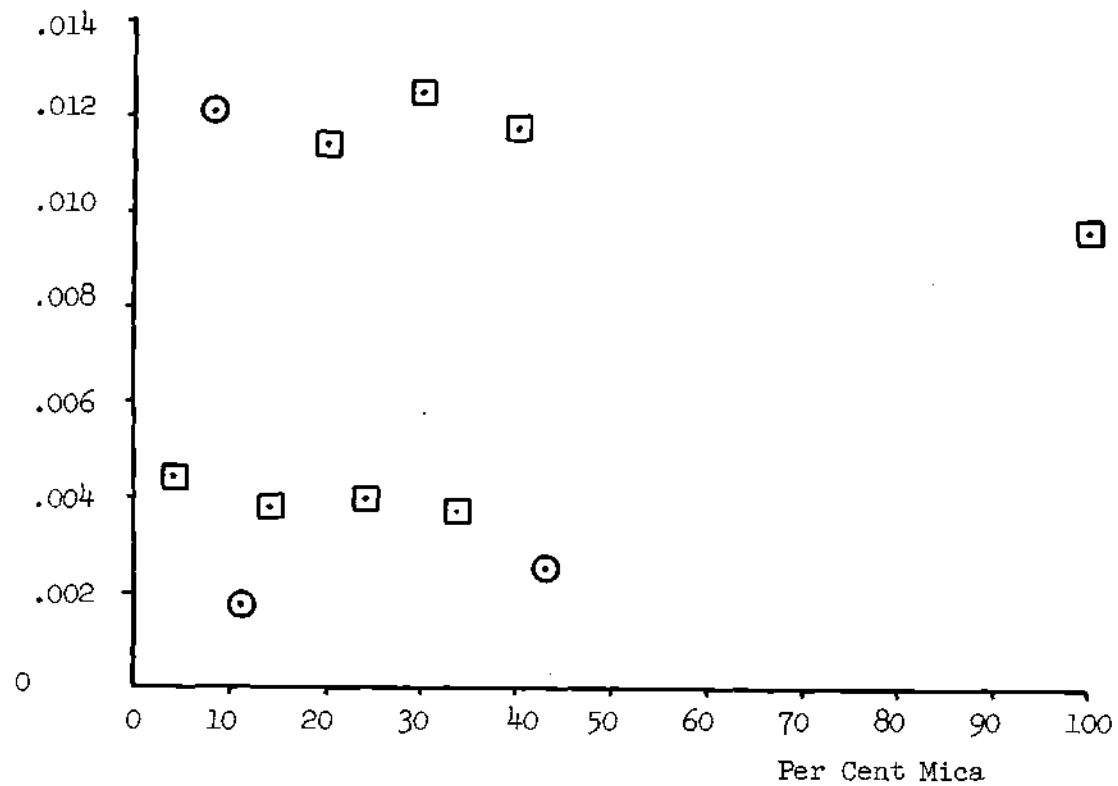


Figure 42. Relationship between Mica Content and the Coefficient of Secondary Compression under 16,000 psf

BIBLIOGRAPHY

1. Clemence, S. P.: "The Effect of Mica Content on the Compressibility of Saprolites," M.S. Thesis, Georgia Institute of Technology, Atlanta, Georgia, 1964.
2. Sowers, G. F.: "Soil and Foundation Problems in the Southern Piedmont Region," Proceedings, American Society of Civil Engineers, Vol. 80, Separate No. 416, 1953.
3. Sowers, G. F.: "Engineering Properties of Residual Soils Derived from Igneous and Metamorphic Rocks," Paper presented at the Second Pan American Conference on Soil Mechanics and Foundation Engineering, Brazil, 1963.
4. Gilboy, G.: "The Compressibility of Sand-Mica Mixtures," Proc., ASCE, No. 54, pp.555-568, 1928.
5. Rubey, W. W., Feld, J., and Krynine, D. P.: Discussion of "The Compressibility of Sand-Mica Mixtures," by G. Gilboy, Proc., ASCE, No. 54, pp. 1933, 2357, and 2543, 1928.
6. Terzaghi, K.: "Influence of Geologic Factors on the Engineering Properties of Sediments," Economic Geology, Fiftieth Anniversary Volume, pp. 570-1, 1955. (Reprinted in Harvard Soil Mechanics Series, Number 50.)
7. Tate, B. D., and Larew, H. G.: "The Effect of Structure on Resilient Rebound Characteristics of Soils in the Piedmont Province of Virginia," Highway Research Record, No. 39, p. 97, Highway Research Board, National Research Council, 1963.
8. McCarthy, D. F., Jr., and Leonards, R. J.: "Compaction and Compression Characteristics of Micaceous Fine Sands and Silts," Highway Research Record, No. 22, p. 23, Highway Research Board, National Research Council, 1963.
9. Buisman, A. S.: "Results of Long Duration Settlement Tests," Proceedings, (First) International Conference on Soil Mechanics and Foundation Engineering, Cambridge, Massachusetts, Vol. 1, p. 103, 1936.
10. Croce, A.: "Secondary Time Effect in the Compression of Unconsolidated Sediments of Volcanic Origin," Proc., 2nd ICSMFE, Rotterdam, Vol. 1, p. 1166, 1948.

11. Peterson, R.: "Studies of Bearpaw Shale at a Dam site in Saskatchewan," Proc., ASCE, Vol. 80, Separate No. 476, p. 476-1, 1954.
12. Adams, J. I.: "The Engineering Behavior of a Canadian Muskeg," Proc., 6th ICSMFE, Toronto, Vol. 1, p. 1, 1965.
13. Sowers, G. F., Williams, R. C., and Wallace, T. S.: "Compressibility of Broken Rock and the Settlement of Rockfills," Proc. 6th ICSMFE, Toronto, Vol. 2, p. 561, 1965.
14. Terzaghi, K.: Erdbaumechanik auf bodenphysikalischer Grundlage, F. Deutche, Vienna, 1925.
15. Gray, H.: "Report on Research on the Consolidation of Fine Grained Soils," Proc., (1st) ICSMFE, Cambridge, Massachusetts, Vol. 2, p. 138, 1936.
16. Housel, W. S.: "Discussion," Proc., (1st) ICSMFE, Cambridge, Massachusetts, Vol. 3, p. 100, 1936.
17. Taylor, D. W.: Research on the Consolidation of Clays, Department of Civil and Sanitary Engineering, Massachusetts Institute of Technology, Serial 82, pp. 42, 52, 53, 1942.
18. Edelman, T.: "Problems of Soil-Settlement," Proc., 2nd ICSMFE, Vol. 1, p. 30, 1948.
19. Terzaghi, K.: "Settlement of Pile Foundations due to Secondary Compression," Proceedings, Fourth Texas Conference on Soil Mechanics and Foundation Engineering, University of Texas, Austin, Part 1, 1941.
20. Terzaghi, K.: "Discussion," Proc., 3rd ICSMFE, Zurich, Vol. 3, p. 158, 1953.
21. Zeevaert, L.: "Foundation Design of Tower Latino Americana in Mexico City," Geotechnique, Vol. 7, No. 3, p. 122, September, 1957.
22. Zeevaert, L.: "Consolidation of Mexico City Volcanic Clay," Special Technical Publication 232, American Society for Testing Materials, pp. 18-32, 1957.
23. Housel, W. S.: "Discussion," Special Technical Publication 232, ASTM, p.381, 1957.
24. Dawson, R. F.: "Settlement Studies on the San Jacinto Monument," Proceedings, 7th Texas Conference on Soil Mechanics and Foundation Engineering, University of Texas, Austin, 1947.
25. Stefanoff, G., Zlaterev, K., Grantcharov, M., and Milev, G.: "Anticipated and Observed Settlement of a High Chimney," Proc., 6th ICSMFE, Toronto, Vol. 2, p. 561, 1965.

26. Newland, P. L., and Allely, G. H.: "A Study of the Consolidation Characteristics of a Clay," Geotechnique, Vol. 10, No. 2, pp. 62-74, 1960.
27. Lo, K. Y.: "Secondary Compression of Clays," Journal of the Soil Mechanics and Foundations Division, Proc., ASCE, Vol. 87, No. SM4, Proc. Paper No. 2885, pp. 61-87, August, 1961.
28. Gibson, R. E., and Lo, K. Y.: "A Theory of Consolidation of Soils Exhibiting Secondary Compression," Acta Polytechnica Scandinavica, Civil Engineering and Building Construction Series No. 10, (C1 10), 296, 1961.
29. Leonards, G., and Girault, P.: "A Study of the One-dimensional Consolidation Test," Proc. 5th ICSMFE, Paris, Vol. 1, p. 213, 1961.
30. Wahls, H. E.: "Analysis of Primary and Secondary Consolidation," J. SMFD, Proc. ASCE, Vol. 88, No. SM6, Proc. Paper No. 3373, pp. 207-231, December, 1962.
31. Madhav, R. M., and Sridharan, A.: "Discussion," J. SMFD, Proc., ASCE, Vol. 89, No. SM4, p. 233, July, 1963.
32. Gray, H.: "Discussion," J. SMFD, Proc., ASCE, Vol. 89, No. SM3, p. 194, May, 1963.
33. Crawford, C. B.: "Interpretation of the Consolidation Test," J. SMFD, Proc., ASCE, Vol. 90, No. SM5, Proc. Paper No. 4056, pp. 87-102, September, 1964.
34. Schmertmann, J. H.: "Discussion," J. SMFD, Proc., ASCE, Vol. 91, No. SM2, p. 131, March, 1965.
35. Taylor, D. W., and Merchant, W.: "A Theory of Clay Consolidation Accounting for Secondary Compression," Journal of Mathematics and Physics, Vol. 19, pp. 167-185, 1940.
36. Naylor, A. H.: "Precise Determination of Primary Consolidation," Proc., 2nd ICSMFE, Rotterdam, Vol. 1, p. 34, 1948.
37. Koppejan, A. W.: "A Formula Combining the Terzaghi Load-Compression Relationship and the Buisman Secular Time Effect," Proc., 2nd ICSMFE, Rotterdam, Vol. 3, p. 32, 1948.
38. Hansen, J. B.: "A Model Law for Simultaneous Primary and Secondary Consolidation," Proc., 5th ICSMFE, Paris, Vol. 1, p. 133, 1961.
39. Hull, A. W.: "A New Method of Chemical Analysis," Journal of the American Chemical Society, Vol. 41, No. 8, pp. 1168-1175, August, 1919.

40. Klug, H. P. and Alexander, L. E.: X-ray Diffraction Procedures, p. 411, J. Wiley, New York, 1954.
41. Alexander, L. E., and Klug, H. P.: "Basic Aspects of X-ray Absorption," Analytical Chemistry, Vol. 20, No. 10, pp. 886-889, October, 1948.
42. Moore, C. A.: "The Use of X-ray Diffraction for the Quantitative Analysis of Naturally Occuring Multicomponent Mineral Systems," Southeastern Geology, Duke University, Durham, Vol. 6, No. 3, pp. 139-158, July, 1965.
43. Konta, J.: "Quantitative Mineralogical Analysis of 'Blue Clay' from Vonsov, Bohemia: A Comparative Study by Nine Laboratories," Clay Minerals Bulletin, Vol. 5, No. 30, pp. 255-264, December, 1963.
44. Grim, R. E.: Clay Mineralogy, McGraw-Hill, New York, 1953.
45. Brown, G. (Ed.): The X-ray Identification and Crystal Structure of Clay Minerals, The Mineralogical Society, London, 1961.
46. American Society for Testing Materials: Index to the X-ray Powder Data File, Special Technical Publication 48-I. 1960.
47. U. S. Waterways Experiment Station: Unified Soil Classification System, Technical Memorandum 3-357, Vicksburg, 1953.
48. Committee on Classification of Materials for Subgrades and Granular Type Roads: "Classification of Soils and Subgrade Materials for Highway Construction," Proc., Highway Research Board, Vol. 25, pp. 376-382, 1945.
49. Sowers, G. F.: Laboratory Manual for Soil Testing, Georgia Institute of Technology, Atlanta, Georgia, 1958.
50. Lambe, T. W.: Soil Testing for Engineers, J. Wiley, New York, 1951.
51. Dana, J. D. (Revised by C. S. Hurlbut, Jr.): Dana's Manual of Mineralogy, 17th Edition, J. Wiley, New York, 1959.
52. Philips Electronic Instruments: Norelco X-ray Analytical Instrumentation, New York, 1963.
53. Vargas, M.: "Some Engineering Properties of Residual Clay Soils Occurring in Southern Brazil," Proc. 3rd ICSMFE, Zurich, Vol. 1, p. 67, 1953.